International Journal of
Geo-Information

MDPI

Article

Groundwater Potential Zone Mapping: Integration of Multi-Criteria Decision Analysis (MCDA) and GIS Techniques for the Al-Qalamoun Region in Syria

Imad Alrawi [1,2], Jianping Chen [1,2,*] and Arsalan Ahmed Othman [3,4]

[1] School of Earth Sciences and Resources, China University of Geosciences (Beijing), Beijing 100083, China
[2] The Key Laboratory of Land Resources Information Research & Development, Beijing 100083, China
[3] Department of Petroleum Engineering, Komar University of Science and Technology, Sulaimaniyah 46001, Iraq
[4] Iraq Geological Survey, Al-Andalus Square, Baghdad 10068, Iraq
[*] Correspondence: 3s@cugb.edu.cn

Abstract: One of the most critical processes for the long-term management of groundwater resources is Groundwater Potential Zonation (GWPZ). Despite their importance, traditional groundwater studies are costly, difficult, complex, and time-consuming. This study aims to investigate GWPZ mapping for the Al-Qalamoun region, in the Western part of Syria. We combined the Multi-Influence Factor (MIF) and Analytic Hierarchy Process (AHP) methods with the Geographic Information Systems (GIS) to estimate the GWPZ. The weight and score factors of eight factors were used to develop the GWPZ including drainage density, lithology, slope, lineament density, geomorphology, land use/land cover, rainfall, and soil. According to the findings, about 46% and 50.6% of the total area of the Al-Qalamoun region was classified as suitable for groundwater recharge by the AHP and MIF methods, respectively. However, 54% and 49.4% of the area was classified as having poor suitability for groundwater recharge by the AHP and MIF methods, respectively. These areas with poor suitability can be utilized for gathering surface water. The validation of the results showed that the AHP and MIF methods have similar accuracy for the GWPZ; however, the accuracy and results depend on influencing factors and their weights assigned by experts.

Keywords: GWPZ; MIF; AHP; Al-Qalamoun; groundwater; GIS

Citation: Alrawi, I.; Chen, J.; Othman, A.A. Groundwater Potential Zone Mapping: Integration of Multi-Criteria Decision Analysis (MCDA) and GIS Techniques for the Al-Qalamoun Region in Syria. *ISPRS Int. J. Geo-Inf.* **2022**, *11*, 603. https://doi.org/10.3390/ijgi11120603

Academic Editors: Godwin Yeboah and Wolfgang Kainz

Received: 30 August 2022
Accepted: 28 November 2022
Published: 2 December 2022

1. Introduction

Groundwater is the most significant natural water resource, and effective groundwater management depends on the quantity and quality of available groundwater. The existence and volume of groundwater depend on the lithological characteristics and the porosity of geological formations [1]. Groundwater moves to discharge locations including springs, streams, lakes, and the sea [2]. As a result, its supply is restricted, and identifying prospective groundwater zones is a considerable challenge in several parts of the world. Climate change affects the quantity of water needed and the supply availability [3]. Groundwater storage is influenced by several factors, such as geological formations, geomorphological structure, porosity, weathering, lineament density, drainage, land use and land cover (LULC), and rainfall [4].

Several studies have used Multi-Criteria Decision Analysis (MCDA) [5–8] and machine learning algorithms [9,10] to estimate the Groundwater Potential Zonation (GWPZ). Remote sensing can investigate large-scale observations of the earth's surface, which makes it a useful tool for GWPZ studies [11]. Furthermore, GIS can effectively manage data in different thematic levels, such as lithology, drainage density, elevation, lineament density, geomorphology, slope, and LULC. All these factors must be considered and integrated accurately when determining the GWPZ [12].

In various regions of the world, several researchers have used MCDA approaches for groundwater studies integrated with remote sensing and GIS techniques [1,4,13–20]. The Multi-Influence Factor (MIF) is a modern MCDA technique for detecting and defining the GWPZ based on specialist opinion [21]. For instance, Bhattacharya et al. [22] used the geospatial approach and MIF technique to allocate the weightage of thematic layers when mapping the GWPZ of the Purulia district, West Bengal. The accuracy of their approach was calculated as 82%. Nag et al. [23] used the same approach to assess the potential groundwater zone in the Khatra Block of the Bankura district, West Bengal. In addition to the MIF method, several studies have used the Analytical Hierarchy Process (AHP), as developed by Saaty [24], to detect and define the GWPZ [25]. The AHP is an MCDM technique for pairwise comparisons of spatial criteria that are assigned weights based on specialist assessment [11,26,27]. It is a common subjective approach that allows users to choose the weight of each criterion when solving problems with many criteria [28,29].

Carefully selecting predictive factors is an important step in MCDA. Several studies have reviewed previous research to select the predictive factors for their models (e.g., [28,30]). In this study, we reviewed 29 recently published, high-quality research papers focusing on GWPZ that were obtained from the Scopus database (Table 1). More than 72.4% of these papers used LULC, drainage density, soil, lithology, slope, lineament density, rainfall, and geomorphology as predictive factors for GWPZ. The remaining factors, which were ignored in this study, were cited in less than 25% of these papers (Table 1).

Several researchers have discovered that combining the AHP and MIF methods with GIS is an efficient and effective GWPZ approach [6,31–38]. Indeed, many scholars have utilized the AHP and MIF approaches to identify the GWPZ by determining the weights of distinct thematic layers and their classes [6,31–38]. By dramatically decreasing the mathematical complexity of decision-making based on methodical expert judgment, the AHP and MIF methodologies have attracted attention as promising tools for groundwater prediction that provide quick, precise, and cost-effective evaluation of groundwater recharge potential [21,39,40].

Nevertheless, other MCDA approaches, such as the certainty factor (CF) and weighted spatial probability modeling (WSPM), are also used in GWPZ studies. For example, Elewa et al. [41] identified the GWPZ in the Sinai Peninsula, Egypt, using Landsat (ETM+) imagery, GIS, watershed modeling system, and WSPM. Yeh et al. [42] used GIS and remote sensing data to find the GWPZs in the Chih-Pen Creek basin in eastern Taiwan.

Table 1. Literature review of the factors used to map potential groundwater zones.

Literature	LULC	Drainage Density	Soil Texture	Lithology	Slope	Lineament Density	Rainfall	Geomorphology	Elevation	NDVI	Groundwater Depth	Distance to River	Aquifer Thickness	Recharge Rate	Pond Density	Sentinel Water Index	Topographic Wetness Index	Soil Depth	Hillshade
[43]	*	*	*	*	*	*		*										*	
[37]	*	*	*	*	*	*	*		*	*			*		*				
[44]	*	*	*	*	*	*	*												
[34]	*	*	*	*	*	*	*	*											
[45]	*	*	*	*	*	*	*	*											
[38]	*	*	*	*	*	*	*	*											
[46]	*	*	*	*	*	*	*	*											
[47]	*	*	*	*	*	*	*	*											
[48]	*	*	*	*	*	*	*	*											
[49]	*	*	*	*	*	*	*	*											
[50]	*	*	*	*	*	*	*	*											
[51]	*	*	*	*	*	*	*	*											
[52]	*	*	*	*	*	*	*	*											
[53]	*	*	*	*	*	*	*	*											
[54]	*	*	*	*	*	*	*	*											
[15]	*	*	*	*	*	*	*	*											
[6]	*		*		*			*	*	*	*								*
[35]	*	*	*	*	*		*		*	*	*			*					
[55]	*	*	*	*	*	*		*											

Table 1. *Cont.*

Literature	LULC	Drainage Density	Soil Texture	Lithology	Slope	Lineament Density	Rainfall	Geomorphology	Elevation	NDVI	Groundwater Depth	Distance to River	Aquifer Thickness	Recharge Rate	Pond Density	Sentinel Water Index	Topographic Wetness Index	Soil Depth	Hillshade
[56]	*	*	*	*			*	*		*							*		
[57]	*	*	*	*	*	*			*	*			*	*		*			
[22]	*	*	*	*	*														
[58]	*	*	*	*	*	*	*	*				*							
[59]	*	*	*		*	*	*	*											
[60]		*		*	*	*						*							
[61]	*	*	*				*	*	*										
[62]	*	*		*		*			*		*								
[63]	*	*	*	*	*		*	*	*		*								
[64]	*	*	*	*	*	*	*												
Average rate%	96.6	96.6	93.1	89.7	89.7	79.3	75.8	72.4	24.1	17.2	13.8	6.9	6.9	6.9	3.5	3.5	3.5	3.5	3.5

The present study was designed to generate a GWPZ map for the Al-Qalamoun region in Syria using the AHP and MIF methods. Although this area suffers from droughts and water scarcity, the Al-Qalamoun region has never been studied before. Therefore, we integrated remote sensing and GIS data to produce high-accuracy GWPZ results. Eight predictive factors were used including drainage density, lithology, slope gradient, lineament density, geomorphology, LULC, rainfall, and soil.

2. Methodology

2.1. Study Area

The study area, Al-Qalamoun, is in the western part of Syria. It covers 1149 km^2 of the Al-Qalamoun Mountain and Eastern Lebanon Mountain series between 36°25′ E–37°0′ E and 34°0′ N–34°15′ N (Figure 1). The temperatures in Al-Qalamoun range between moderate in the summer and cold in the winter. The coldest temperatures range from about 1 °C to 15 °C, whereas the highest temperatures range from about 22 °C to 41 °C. These temperatures are typical for areas located between an altitude of 846 and 2598 m above sea level. The study area represents a desert region with an average annual rainfall ranging between 111 and 430 mm. The groundwater level in the study area ranges from 30 to 530 m [65].

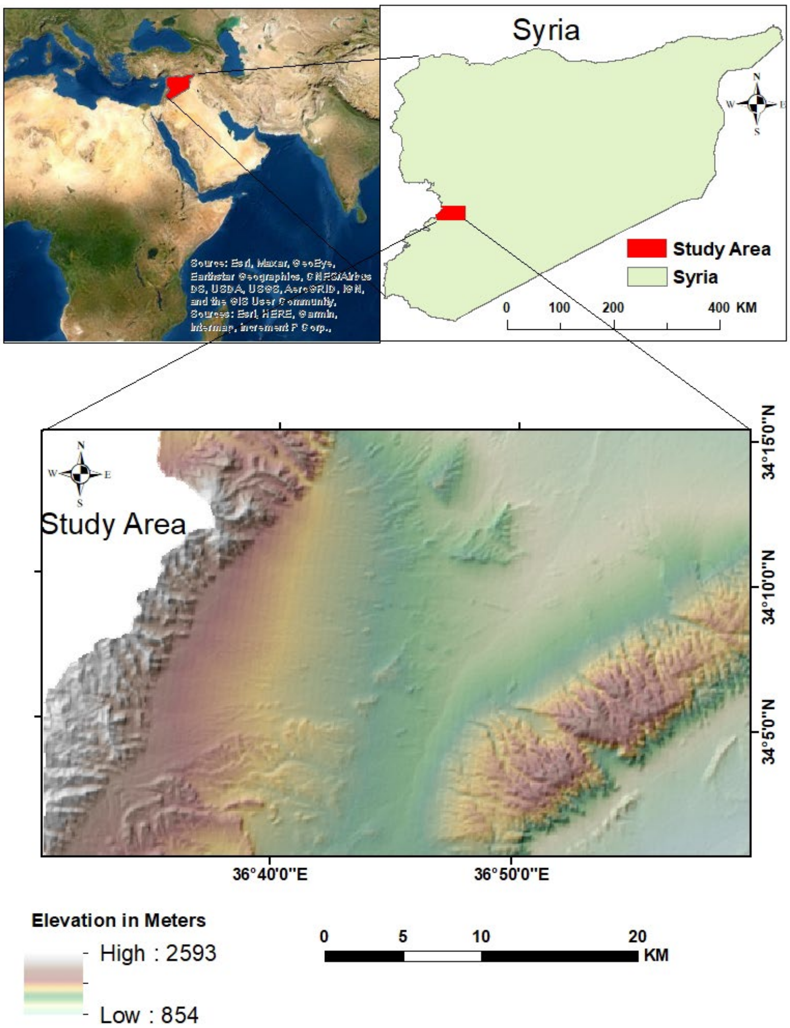

Figure 1. The study area of Al-Qalamoun.

The lithology of the study area is mainly chalky and nummulitic limestone followed by calcareous sandstones, dolomites, and quaternary sediments (i.e., conglomerates and sandstones) [66]. The soil types are mainly aridisols and entiosols [67]. Agriculture, which is considered the main economic activity in the area, uses both surface water and groundwater. Therefore, water resource management is a considerable issue that must be addressed in the Al-Qalamoun region.

2.2. Factors Used for Modeling

The MIF and AHP methods, GIS, and remote sensing techniques were integrated to map the GWPZ. We used the following factors for modeling: lithology, lineament density, LULC, drainage density, slope, geomorphology, rainfall, and soil. The lithology map of the study area was prepared using a hardcopy of the geological map obtained from the Department of Geological Survey and Mineral Research of Syria (1: 200,000 scale) [68]. The soil map was prepared using the soil map of the Arab Center for the Studies of Arid zones and Dry Lands (ACSAD) (1: 1,000,000 scale) [69]. The geomorphology map of the study area was created by digitizing the geomorphologic map of Syria published by the Department of Geological Survey and Mineral Research of Syria (1:1,000,000 scale) [70]. The three maps (lithology, soil, and geomorphology) were scanned with 400 dpi and digitized manually in ArcMap. The Digital Elevation Model (DEM) of the Shuttle Radar Topographic Mission (SRTM), including 30 m spatial resolution data, was obtained from the EarthExplorer website [71] and used to extract the drainage pattern and the slope gradient and prepare the drainage density of the study area. The faults were not well identified in the large-scale geological map (1: 200,000 scale) of the study area. Therefore, we extracted the lineaments using the DEM and the Landsat 8 satellite imagery acquired from the EarthExplorer website [71] on 24 June 2021 (Path: 174 and Row: 036) with 30 m spatial resolution. The Landsat 8 OLI satellite imagery was also used to prepare the LCLU map. The LCLU map was verified with fieldwork, for the accessible areas, and Google Earth, for the inaccessible areas. Meteorological station data were not available for the study area. Therefore, we used CHIRPS rainfall data, which is used in several types of research [72–77]. The CHIRPS data has a spatial resolution of 0.5 degrees and a temporal resolution of the daily, monthly, pentad, decadal, annual, and temporal domains (1981—present) [76]. The rainfall data for 18 points distributed over the entire study area were collected from the Food and Agriculture Organization (FAO) of the United Nation online platform [78] (https://wapor.apps.fao.org) for the years 2009 to 2019. We interpolated these points with a spatial resolution of 30 m to create a map using the Inverse Distance Weight (IDW) technique in ArcGIS. To validate the observed precipitation data, we compared the CHIRPS rainfall dataset with data obtained from the Al-Nabek and Qara meteorological stations. Forty-eight monthly precipitation measurements, covering the period from October 2009 to September 2013, were compared with the CHIRPS data (Figure 2). The result showed a strong correlation, where the coefficients of determinations (R^2) were >0.97 and the *p*-values were <0.05.

2.3. Statistical Models

We used the MIF and AHP methods to analyze the model factors and derive their rating score. The GWPZ was then estimated using the factor weightage and rank. The final GWPZ was created using overlay analysis.

This study used eight main factors (i.e., lithology, lineament density, LULC, drainage density, slope, geomorphology, rainfall, and soil) to identify the GWPZ. We tested 10 models: five models for the MIF method and five models for the AHP method. In each model, we used different weights for each factor (Appendix A: Tables A1–A5). The significance score of the utilized factors was also determined using the MIF and AHP methods. We used both the MIF and AHP methods five times with different impacts and weights assigned to each factor. As a result, five maps were obtained for each method (Figure 3).

The results were validated using the groundwater level data, and the GWPZ was identified by combining all the thematic layers using the weighted overlay analysis method in ArcGIS 10.8. The GWPZ map was then classified into five classes using the natural breaks (Jenks) classification method. We named the classes very high, high, moderate, low, and very low (Figure 4).

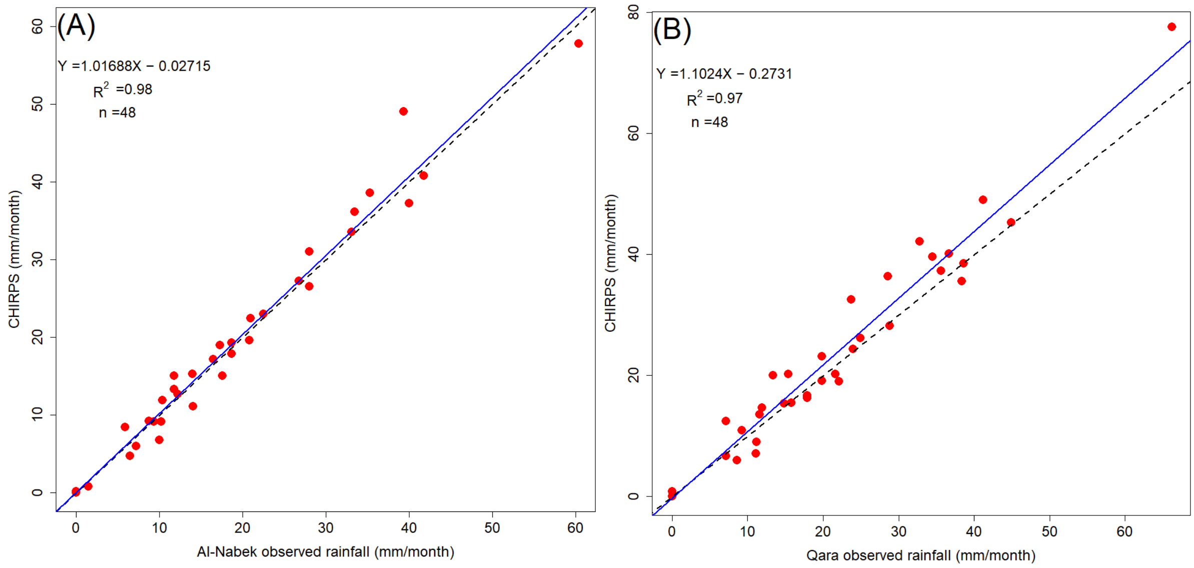

Figure 2. The linear correlation between the CHIRPS data and the precipitation data obtained from (**A**) Nabek and (**B**) Qara stations for the period between October 2009 and September 2013.

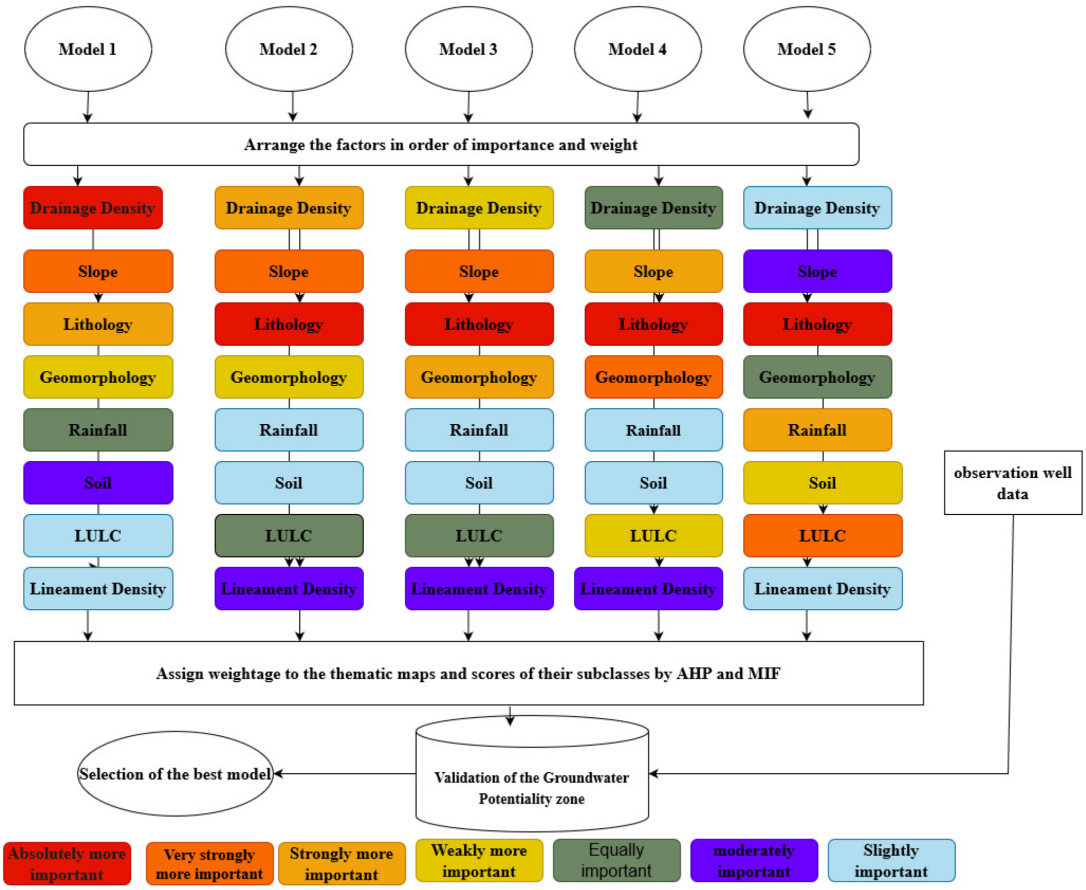

Figure 3. Flow chart of the methodology used to select the best model.

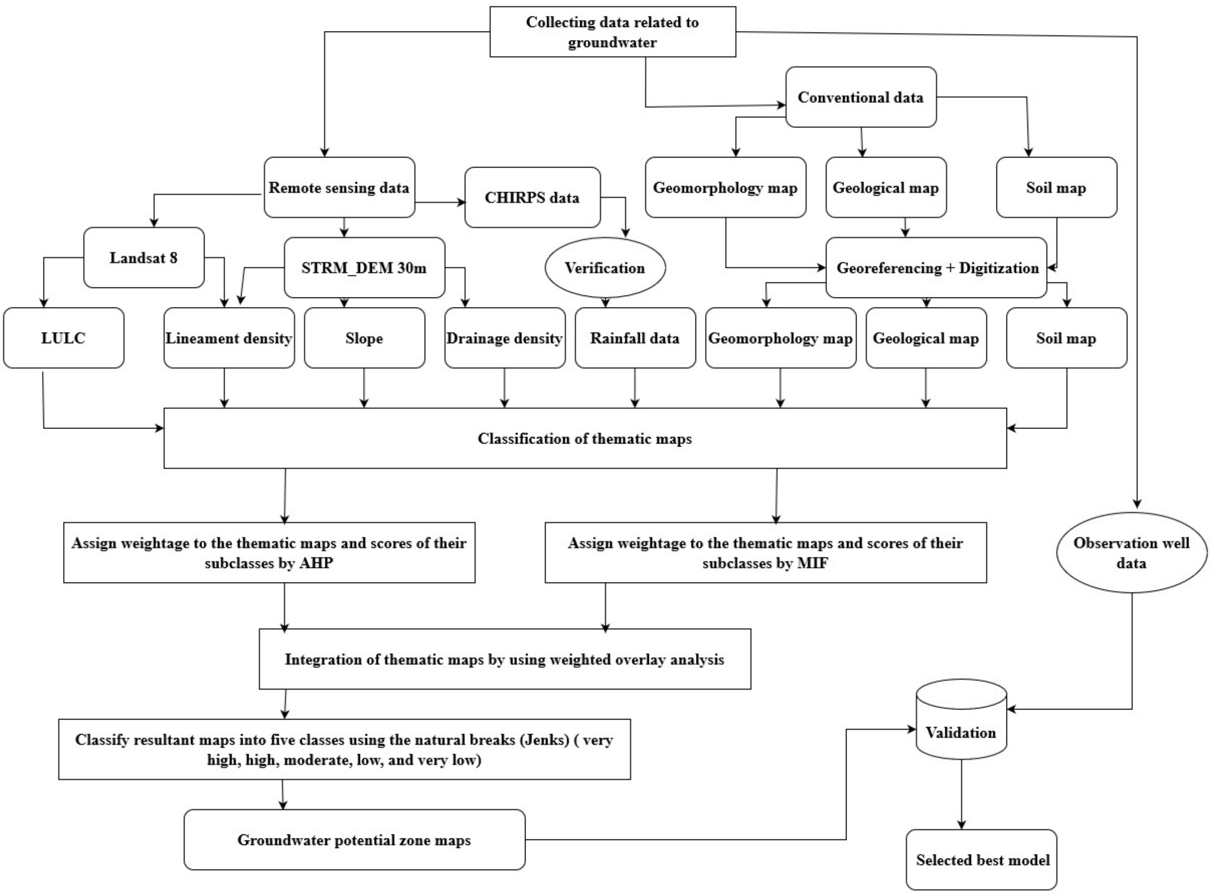

Figure 4. Flow chart of the methodology used to select the best model.

2.3.1. Multi-Influence Factor (MIF) Techniques and Groundwater Potential Zone Method

Weights were assigned to each factor based on their relevance using the MIF approach. The primary and secondary interactions between the variables that influence the GWPZ were used to generate the rankings [21]. The MIF method is very effective and exact for estimating the weights of influential parameters [43]. Table 2 lists the weight scores, where a 1.0 weight score is assigned to each main factor and a 0.5 weight score is assigned to each minor factor [21,22,27]. After assigning weights, the proposed relative rates for groundwater potentiality were computed based on the minor and major consequences of each factor. In this analysis, the significance of each factor was estimated based on published literature and the author's knowledge of the hydrogeological conditions in the study area. Finally, as illustrated in equation 1 [6,11,35–37,44,64], the relative score was utilized to derive the suggested score of individual factors:

$$S_i = \frac{j+n}{\sum(j+n)} \times 100 \quad (1)$$

where S_i is the proposed score of a factor and j and n are the major and minor effect factors, respectively.

After calculating the score for each factor, we allocated the ranks (R_i) of each sub-class of each factor. The first sub-class had the most important influence and received the same rank as the factor score ($R_i1 = S_i$) [35]. The rank of the second sub-class (R_i2) was calculated by dividing S_i by the total number of subclasses (n) and subtracting the resultant value (V_i) from R_i1 (i.e., second sub-class (R_i2) Equation (2)) [35,37,79]. The rank of the third sub-class (R_i3) was calculated by subtracting V_i from R_i2. The ranking process was repeated for all successive sub-classes (Table 2). For example, if the weight of the factor is 20, the first sub-class of the of the factor is also 20, and the number of the subclasses (n) of a given factor are 5 the results will be 16 (i.e., 20–(20/5) = 16). Equation (2) was defined as:

$$R_i 2 = R_i 1 - \left(\frac{S_i}{n}\right) \quad (2)$$

where S_i is the factor score, R_i is the rank of a sub-class of the factor, $R_i 1$ is the rank of the first sub-class, $R_i 2$ is the rank of the second sub-class, and n is the number of sub-classes of the given factor.

Finally, the $GWPZ$ map was created by calculating the raster using Equation (3) [21,35,44]:

$$GWPZ = \sum_{i=1}^{n} (S_i \times R_i) \quad (3)$$

where $GWPZ$ is the groundwater potential zone, S_i is the score of each factor, and R_i is the rank of each sub-class of a given factor, mentioned above.

Table 2. MIF weight scores for groundwater potential zone mapping.

Factors	Major Effect (j)	Minor Effect (n)	Proposed Relative Rate (j + n)	Proposed Score
Lithology	1 + 1 + 1 + 1	0.5	4.5	20
Slope	1 + 1 + 1	0.5 + 0.5	4	18
Drainage Density	1 + 1 + 1	0.5	3.5	15
Geomorphology	1 + 1	0.5 + 0.5	3	13
LULC	1 + 1	0.5	2.5	11
Lineament Density	1 + 1	0.0	2	9
Rainfall	1	0.5	1.5	7
Soil	1	0.5	1.5	7
Total			$\sum(j+n)$ = 22.5	100

2.3.2. Analytical Hierarchy Process (AHP) Techniques and Groundwater Potential Zone Method

Saaty introduced the AHP approach in a series of articles [24,80,81]. The AHP approach works by constructing a set of pairwise comparison matrices that are used to compare all the important elements. This pairwise assessment of the relevance of distinct criteria and sub-criteria inside the judgment matrix converts the MCDA issue into a hierarchy [82,83]. The AHP approach compares the weight and relevance of each factor to the other factors and yields an overall weight for each relevant factor [36,84]. The hierarchy enables the identification of the GWPZ from competing sets of factors by considering each of the numerous features independently. In this work, we identified the GWPZs in the Al-Qalamoun study area by applying the AHP method to eight thematic layers that influence the occurrence of groundwater, including lithology, lineament density, drainage density, LULC, slope, soil, rainfall, and geomorphology. For the pairwise comparisons, each factor was given a score between 1 and 9 based on its relevance relative to other factors (Table 3) using a conventional Saaty's 1–9 scale [24] (Table 4).

The relative weight of each criterion was calculated by normalizing the eigenvectors of each matrix member as shown in Table 5. The Consistency Index (CI) and Consistency Ratio (CR) were used to assess the consistency of the matrix. The CI and CR were calculated using Equations (4) and (5):

$$\mathrm{CI} = \frac{\lambda_{max} - n}{n - 1} \quad (4)$$

$$CR = \frac{\mathrm{CI}}{\mathrm{RI}} \quad (5)$$

where CI is the consistency index, λ_{max} is the greatest Eigenvalue of a matrix, n is the number of factors, CR is the consistency ratio, and RI is the Random Index value. RI was computed by Saaty based on the number of factors [80] (Table 5). The consistency of the matrix can be accepted if the CR is less than 0.1 [85].

Table 3. Pairwise comparison matrix for all factors.

Factors	LI	SLP	DD	GM	LULC	LD	RN	SL
Lithology (LI)	1	2	3	3	5	5	7	9
Slope (SLP)	1/2	1	2	3	3	5	5	7
Drainage (DD	1/3	1/2	1	3	3	3	5	5
Geomorphology (GM)	1/3	1/3	1/3	1	2	3	4	5
Land use and Land cover (LULC)	1/5	1/3	1/3	1/2	1	3	5	5
Lineaments (LD)	1/5	1/5	1/3	1/3	1/3	1	2	3
Rainfall (RN)	1/7	1/5	1/5	1/4	1/5	1/2	1	3
Soil (SL)	1/9	1/7	1/5	1/5	1/5	1/3	1/3	1
SUM	2.82	4.71	7.40	11.28	14.73	20.83	29.33	38

Table 4. Conventional Saaty's scale used in the AHP method [24].

Scale for Importance	Scale
Equally important (EI)	1
Weakly more important (WMI)	3
Strongly more important (SMI)	5
Very strongly more important (VSMI)	7
Absolutely more important (AMI)	9
Intermediate scale	2,4,6,8

Table 5. Identifying the standardized weights for influencing factors in GWPZ.

Factor	LI	SLP	DD	GM	LULC	LD	RN	SL	Weight	Weight %
LI	0.35	0.43	0.40	0.27	0.34	0.24	0.24	0.24	0.31	31
SLP	0.18	0.21	0.27	0.26	0.20	0.24	0.17	0.18	0.21	21
DD	0.12	0.11	0.13	0.27	0.20	0.15	0.17	0.13	0.16	16
GM	0.12	0.07	0.05	0.09	0.14	0.14	0.14	0.13	0.11	11
LULC	0.07	0.07	0.04	0.04	0.07	0.14	0.17	0.13	0.09	9
LD	0.07	0.04	0.05	0.03	0.02	0.05	0.07	0.08	0.05	5
RN	0.05	0.04	0.03	0.02	0.02	0.02	0.03	0.08	0.04	4
SL	0.04	0.03	0.03	0.02	0.01	0.02	0.01	0.03	0.03	3
SUM	1	1	1	1	1	1	1	1	1	1
n	1	2	3	4	5	6	7	8	9	10
RI	0	0	0.58	0.90	1.12	1.24	1.32	1.41	1.49	1.51

λ_{max} = 8.517, n = 8, CI =0.0739, RI = 1.41, and CR = 0.0524 < 0.1.

Each sub-class of a thematic map was given a rank of 1–5 based on its effect on the occurrence of groundwater [86–89]. The rankings indicated the following effects: 1 = very low, 2 = low, 3 = moderate, 4 = high, and 5 = very high. Every thematic layer was given a weight, and every sub-class of each factor was given a rank (Table 6). Finally, the GWPZ map was created using Equation (6) [47,51,58,90], in the ArcGIS 10.8 environment:

$$\text{GWPZ} = LI_w LI_r + LD_w LD_r + SL_w SL_r + RN_w RN_r + LU/LC_w LU/LC_r + DD_w DD_r + SLP_w SLP_r + GM_w GM_r \quad (6)$$

where GWPZ is the Groundwater Potential Zonation, LI is the lithology, LD is the lineament density, SL is the soil, RN is the rainfall, $LULC$ is the land use/land cover, DD is the drainage density, SLP is the slope, and GM is the geomorphology. In addition, the "w" and "r" are the weight and rank of a given factor, respectively.

Table 6. Weight and scores of specific characteristics that were assigned to factors that influence GWPZ.

Factors	Sub-Classes	MIF		AHP	
		Weight	Score	Weight	Rank
Lithology	Quaternary sands, loams	20	20	31	9
	Quaternary conglomerates, sandstones, loams		16		7
	Cretaceous limestone, marl dolomites		12		5
	Neogene limestone, conglomerates, sands		8		3
	Paleogene Chalky limestone, marls		4		1
Slope	80–87	18	2	21	1
	60–80		6		3
	40–60		10		5
	20–40		14		7
	0–20		18		9
Drainage Density	Very Low	15	15	16	9
	Low		12		7
	Medium		9		5
	High		6		3
	Very High		3		1
Geomorphology	Flood plain	13	13	11	9
	Upper quaternary and recent alluvial fans		10		7
	Low mountains with small and low ridges		7		5
	Desert weathering outliers		4		3
	Low mountains with coniform and cuesta-hilly relief		1		1
	Medium-height mountains with flattened divides and steep abrupt slopes		1		1
LULC	Built-Up Land	11	3	9	1
	Bare Mountain		5		3
	Barren Land		7		5
	Pasture Land		9		7
	Agriculture Land		11		9
Lineament Density	Very Low	9	1	5	1
	Low		3		3
	Medium		5		5
	High		7		7
	Very High		9		9
Rainfall (mm)	270–430	7	7	4	9
	197–270		6		7
	163–197		5		5
	139–163		4		3
	111–139		3		1
Soil	Entisols-Lithic Torriorthents, Coarse and medium—Orthids, level to Steep.	7	7	3	9
	Entisols-Lithic Torriorthents, Coarse and medium—Rock outcrop, steep.		6		7
	Aridisols-Typic Camborthids, medium—Typic Calciorthids, Level.		5		5
	Aridisols-Typic Paleorthids, Coarse and medium-level sloping and steep.		4		3
	Aridisols-Typic Calciorthids, Coarse—Paleorthids, Sloping.		3		

2.4. Validation

To validate the GWPZ maps, we used the area under the curve (AUC) of the Receiver Operating Characteristics (ROC) method. This method has been widely applied by several researchers [38,43,44,91–93]. In this study, we compared the suitability of the MIF and AHP methods for creating GWPZ maps using the area under the curve (AUC) of the Receiver Operating Characteristics (ROC) [44,94]. The ROC plots show the relationship between the cumulative areas under different groundwater zones and the cumulative number of wells available in each potential region [43]. Data from a total of 22 wells were used to evaluate the accuracy of the GWPZ maps produced by the MIF and AHP methods. Most of the wells produced groundwater at an acceptable rate ranging between 35–55 m^3/h. We used the ROC to select which method is the best for GWPZ mapping [6,95].

3. Results and Discussion

3.1. Evaluation of Predictive Factors

The GWPZs in the study area were estimated using eight factors: lithology, drainage density, slope, lineament density, LULC, geomorphology, rainfall, and soil. Figure 5c shows the lithological units of the study area, which are useful for determining the hydrogeological properties of rocks. The lithology includes Cretaceous limestone, marl dolomites (31%); Neogene limestone, conglomerates (3%), sands; and Paleogene Chalky limestone, marls (22%). In total, 44% of the area was covered by Quaternary conglomerates, sandstones, and loams (where Quaternary sands, loams accounted for 43% and Quaternary conglomerates, sandstones, loams accounted for 1%). The Quaternary conglomerates, sandstones, and loams are the most important aquifer in the basin. The MIF score of the sub-classes ranged from 4 to 20, whereas the AHP score of the sub-classes ranged from 31 to 279. The weightage of the lithology factor was 20 in the MIF method and 31 in the AHP method. A higher importance was given to Quaternary conglomerates, sandstones, and loams based on field investigation and their aquifer system. The rating and weightage of the lithology factor are listed in Table 6.

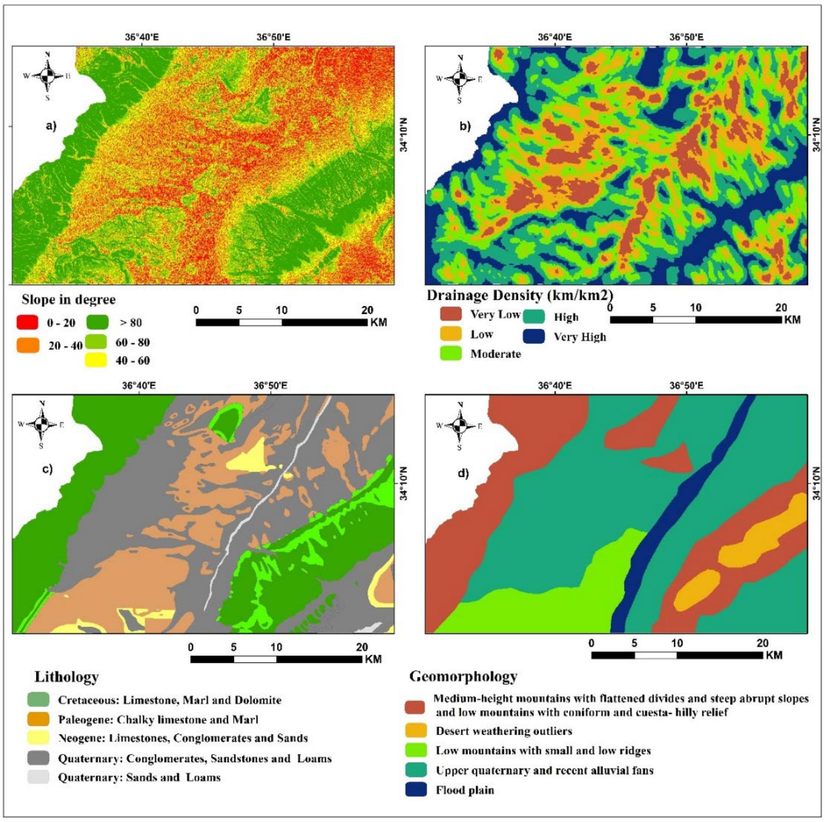

Figure 5. (**a**) Slope, (**b**) Drainage density, (**c**) Lithology, and (**d**) Geomorphology.

Low groundwater recharge occurs in media with a high drainage density, and high groundwater recharge occurs in media with a low drainage density [11,14,42]. Therefore, drainage density is one of the most important indicators of hydrogeological characteristics [34]. Permeability is inversely proportional to the drainage density [44,96]. The drainage density of the study area is classified into five classes: very low (10%), low (20%), medium (26%), high (27%), and very high (17%) (Figure 5b). The very low drainage density has a high infiltration rate. Thus, the high score was assigned to very low drainage density. The overall score for the drainage density factor ranged from 3 to 15 and 16 to 144 when calculated using the MIF and AHP methods, respectively. Table 6 shows the MIF and AHP weight and score of the drainage density factor.

The slope of an area is among the factors that regulate water permeation into the subsurface. Surface water infiltration does not occur in the same spot everywhere. In smooth slope areas, surface water runoff is weak and infiltration is high. In high-slope areas, surface water runoff is strong and infiltration is low [11,14]. The slope of the study area ranged from 0° to 87° (Figure 5a). Areas with the lowest slope, ranging from 0–20° (13.5%), were given the highest weight due to low runoff and high infiltration. The overall score of the slope factor is listed in Table 6.

The geomorphology features of the study area were floodplain (5%), Upper Quaternary and recent alluvial fans (52%), low mountains with small and low ridges (11%), desert weathering outliers (4%), low mountains with conform and cuesta- hilly relief, and medium-height mountains with flattened divides and steep abrupt slopes (28%) (Figure 5d). For GWPZ, the highest importance was given to the floodplain region due to the high amount of infiltration. All scores for the geomorphology factor ranged from 1 to 13 and 11 to 99 when calculated using the MIF and AHP methods, respectively (Table 6).

Rainfall is the primary source of recharge for aquifer units [38,44,97]. As a result, the possibility of GWPZs grows as rainfall distribution changes. The rainfall in the study area ranged from 111 to 430 mm (Figure 6a). The highest rainfall areas had a higher amount of GWPZ. The areas with 270 to 430 mm (19%) of rainfall areas were assigned high weightage. The overall score of the rainfall factor ranged from 7 to 3 and 4 to 36 when calculated using the MIF and AHP method, respectively (Table 6).

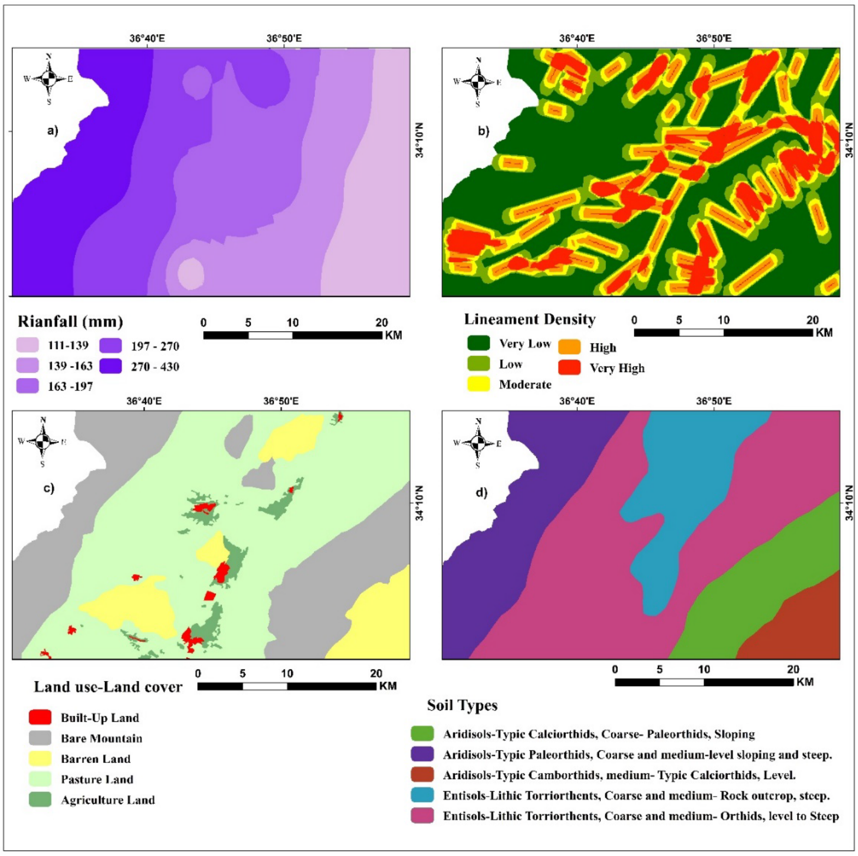

Figure 6. (**a**) Rainfall, (**b**) Lineament density, (**c**) LULC, and (**d**) Soil.

The rate of infiltration is determined by the porosity of the soil type [98], which is controlled by the amount of groundwater recharge. The soil types of the study area are listed in Table 6. Based on the infiltration rate of each soil, the highest overall score was assigned to type Entisols-Lithic Torriorthents, Coarse and medium- Orthids, level to Steep based. Figure 6d shows a soil map of the study area.

The LULC shows the surface of the earth. The LULC of the study area consists of built-up land (1%), bare mountains (30%), barren land (12%), pastureland (54%), and agricultural land (3%; Figure 6c). According to [22,35,38,40,99–101], agricultural land decreases the speed of surface water runoff, which raises water infiltration. Therefore, priority has been given to determining the groundwater potential zone of agricultural land. The overall weightage of LULC was 11 and 9 when calculated using the MIF and AHP methods, respectively. Table 6 shows the score and weightage values for each of the LULC sub-classes as calculated using the MIF and AHP methods.

Lineaments are a type of subterranean geological feature (fractures or structures) that can be discovered through remote sensing [102,103]. Groundwater yields in regions where lineaments parallel to drainage networks intersect can be higher than in other areas. As a result, lineaments provide information about groundwater transport and storage, as well as aid in the identification of groundwater zones in hydrogeological studies [104]. The lineament density in the study area is classified into five classes ranging from extremely low (48%) to very high (14%; Figure 6b). As shown in Table 6, the overall score of the lineament factor ranged from 1 to 9 and 5 to 45 when calculated using the MIF and AHP methods, respectively. The areas with high lineament density were given high importance for GWPZ because of their high infiltration.

3.2. Groundwater Potential Zonation

Many researchers have discovered that combining the AHP and MIF methods with GIS is an efficient and effective GWPZ approach. The AHP and MIF methods have been used to identify the GWPZ by determining the weights of distinct thematic layers and their classes [8,28–35]. By dramatically decreasing the mathematical complexity of decision-making based on methodical expert judgment, the AHP and MIF methods have attracted attention as promising tools for quick, precise, and cost-effective evaluation of groundwater recharge potential [21,39,40].

The GWPZ map of the study area was created utilizing GIS-based MIF, AHP, and overlay analyses of the factors that were identified as important groundwater predictors in our literature review (Appendix A: Figures A1–A5). To begin, the MIF and AHP methods were utilized to calculate the weight values of the factors and the score values of each sub-class. The score and weightage of each factor was multiplied and attributed to the respective raster file of the factors.

The AHP method classified the GWPZ of the study area as follows: very high, 182 km^2 (16%); high, 253 km^2 (22%); moderate, 178 km^2 (16%); low, 302 km^2 (26%); and very low, 229 km^2 (20%). In contrast, the MIF method classified the GWPZ of the study area as follows: very high, 180 km^2 (16%); high, 265 km^2 (23.2%); moderate, 260 km^2 (22.8%); low, 243 km^2 (21%); and very low 194 km^2 (17%). The Qara, Alhafar, and Alsehel regions were mainly in very high and high GWPZ, whereas the Al-Nabek area was in moderate potential areas. Other parts of the study area were covered by low and very low potential zonation. Figure 7 shows the GWPZ maps of the study area created by using the MIF and AHP methods.

Several researchers have found that the GWPZ map produced using the AHP approach is more efficient than that produced using the MIF technique [6,35,38,56]. However, others have found that using the MIF technique is more efficient than using the AHP method [36,37,44,57]. In this study, we found that the quality of a GWPZ map produced using the AHP and MIF methods depends on the thematic layers that are used and the impact and weights assigned by experts. Even small modifications in layer weightings and techniques can have a major influence on the findings. As a result, the importance of the thematic layers and their effect in defining the GWPZ should take precedence over the method used. In MCDA, the subjective attitude of scientists when choosing the influence of individual factors and weights affects the result of the models. Therefore, careful consideration of predictive factors is required to adequately assess the weightings of these factors according to specific site conditions [28,30]. Moreover, the weights for each factor must be precise. Weight values can be obtained from previous studies that investigated areas with similar climate conditions. However, the researcher should ignore outliers and nonlogical factors and weights of factors used by some of the articles.

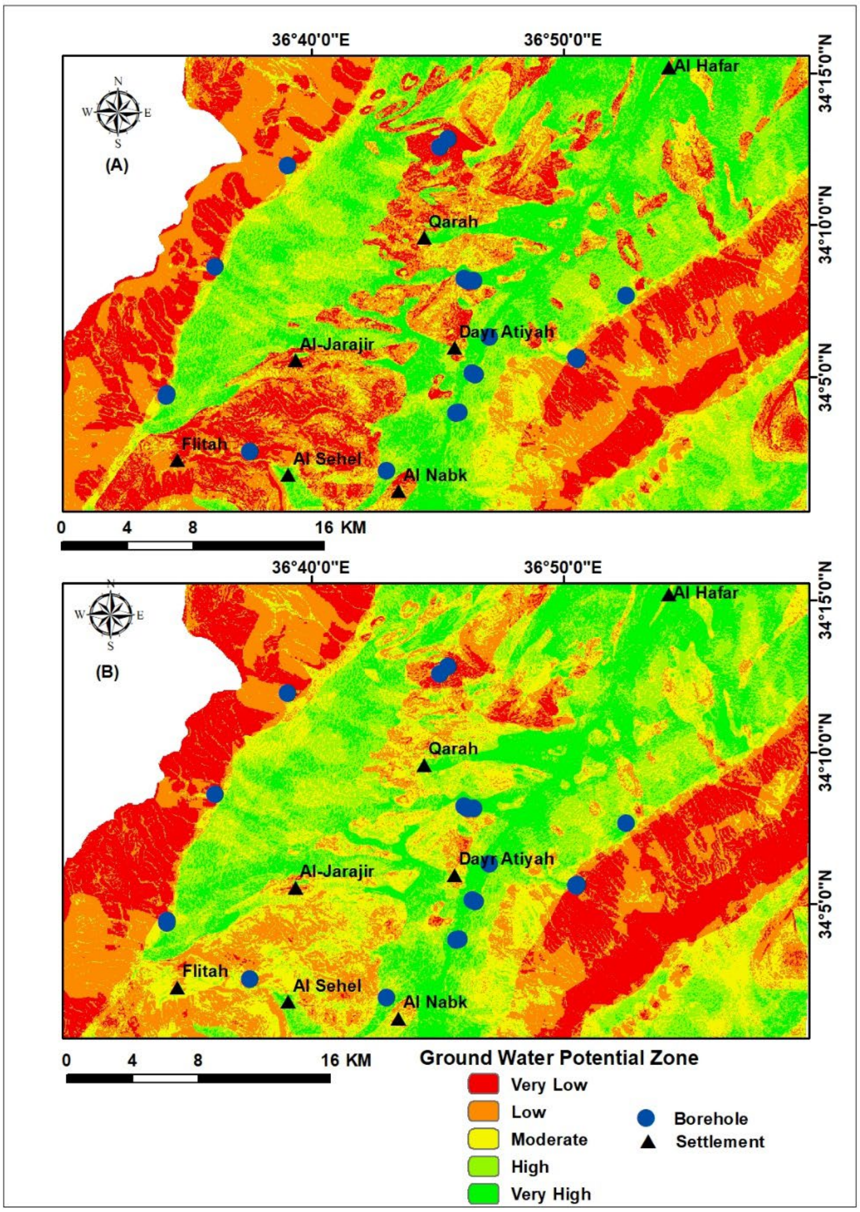

Figure 7. Groundwater Potential Zone of (**A**) AHP and (**B**) MIF maps.

3.3. Validation

Validation of results is one of the most crucial steps in determining the correctness of any model. Models are not very relevant from a scientific standpoint without a validation [43,105]. Various methods are used to validate GWPZ maps, such as receiver operating characteristics (ROC) analysis, the area under the curve (AUC), and correlation analysis (R^2) [6,35,36,43,106,107]. We validated the accuracy of the ten GWPZ models obtained with the MIF and AHP methods using data from 22 wells (Figure 8) by scheming the accumulative regions under different groundwater potential zones and the cumulative percentage number of wells located in each potential zone. The area under the curve (AUC) was calculated using the graph. A good model typically has an AUC value between 0.6 and 0.8, whereas an outstanding model typically has values over 0.9 [44,56]. Our ROC analysis results indicated that areas under the curves (AUC) of the models were 62.16%, 60.86%, and 68.93%, 64.11% for MIF1, AHP1, and MIF5 and AHP5, respectively. The results for model 1 and model 5 showed that the MIF method is better than the AHP method [36,37,57]. However, the results of the ROC analysis for model 3 indicated that the AHP is more suitable than the MIF method for GWPZ [6,35,44,56], according to the AUC values of 66.15%, 62.40% for AHP3 and MIF3, respectively. For model 2 and model 4, the results of the ROC showed that the AHP and MIF methods produced GWPZ maps of similar quality, according to the AUC values of 67.51%, 67.65%, 69.85%, and 69.86% for AHP4, MIF4, AHP2, and MIF2, respectively. In this study, we adopted the second model for each of the two methods (MIF2 and AHP2), as indicated in Table 6.

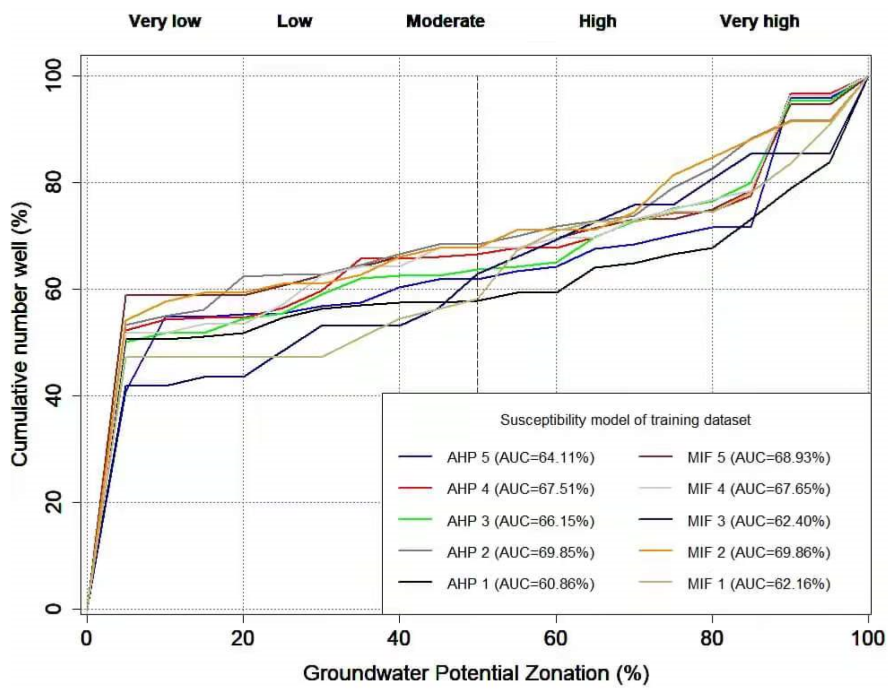

Figure 8. Results of the ROC for validation of groundwater potential maps using the AHP and MIF methods.

This study is important for the long-term groundwater management of the study region. However, future work is required to improve groundwater management.

4. Conclusions

The Al-Qalamoun region was used in this study to map the GWPZ using the MIF and AHP methods based on GIS. To determine potential zones, several factors were considered and analyzed, including lineament density, lithology, LULC, drainage density, soil, slope, rainfall, and geomorphology. Remote sensing techniques were also used to construct geomorphology, LULC, slope, lineament density, and drainage density maps for the research area. The weight and score values of each factor were determined using the Multi Influence Factor approach. The GWPZ was calculated using the weight and rating values for each factor, and very high, high, moderate, low, and very low GWPZ were used to classify the study region into five categories. The validation of the results shows that the AHP and MIF methods have similar accuracy for GWPZ. However, the accuracy of the results depends on the model used and on the influencing factors and their weights.

The findings of this study are critical for the long-term management of the study region and the use of groundwater by local governments. Our results will also be beneficial for watershed planners and appropriate watershed management, notably in water budgeting initiatives. Moreover, based on the validation for the MCDA (i.e., the AHP and MIF methods) models, it appears that all models perform equally well, and the focus should be on the careful selection of the factors, which is far more important than the methods used.

For future work, we strongly recommend using evaporation and temperature factors to select the GWPZ. These factors were not considered in our analysis due to the lack of data within the study area. Furthermore, we advise testing the machine learning algorithms, such as random forests, support vector machine, and artificial neural network, when the required data are available. Machine learning algorithms might give a better result.

Author Contributions: Imad Alrawi: writing—original draft, Arsalan Ahmed Othman and Jianping Chen: writing—review and editing. All authors have read and agreed to the published version of the manuscript.

Funding: This research was funded by No. 2017YFC0601502 from the National Key Research and Development Program of China.

Institutional Review Board Statement: Not applicable.

Informed Consent Statement: Not applicable.

Data Availability Statement: All data generated or analyzed during this study are included in this published article.

Conflicts of Interest: The authors declare no competing interests.

Appendix A

Table A1. Weight and scores of specific characteristics in (MIF1 and AHP1) are assigned to factors that influence GWPZ.

Factors	Sub-Classes	MIF1		AHP1	
		Weight	Score	Weight	Rank
Drainage Density	Very Low	20	20	35	9
	Low		16		7
	Medium		12		5
	High		8		3
	Very High		4		1
Slope	80–87	18	2	19	1
	60–80		6		3
	40–60		10		5
	20–40		14		7
	0–20		18		9
Lithology	Quaternary sands, loams	15	15	16	9
	Quaternary conglomerates, sandstones, loams		12		7
	Cretaceous limestone, marl dolomites		9		5
	Neogene limestone, conglomerates, sands		6		3
	Paleogene Chalky limestone, marls		3		1
Geomorphology	Flood plain	13	13	10	9
	Upper quaternary and recent alluvial fans		10		7
	Low mountains with small and low ridges		7		5
	Desert weathering outliers		4		3
	Low mountains with coniform and cuesta—hilly relief		1		1
	Medium-height mountains with flattened divides and steep abrupt slopes		1		1

Table A1. *Cont.*

Factors	Sub-Classes	MIF1		AHP1	
		Weight	Score	Weight	Rank
Rainfall (mm)	270–430	11	3	10	9
	197–270		5		7
	163–197		7		5
	139–163		9		3
	111–139		11		1
Soil	Entisols-Lithic Torriorthents, Coarse and medium-Orthids, level to Steep.	9	9	5	9
	Low Entisols-Lithic Torriorthents, Coarse and medium-Rock outcrop, steep.		7		7
	Aridisols-Typic Camborthids, medium- Typic Calciorthids, Level.		5		5
	Aridisols-Typic Paleorthids, Coarse and medium-level sloping and steep		3		3
	Aridisols-Typic Calciorthids, Coarse- Paleorthids, Sloping.		1		1
LULC	Built-Up Land	7	3	3	1
	Bare Mountain		4		3
	Barren Land		5		5
	Pasture Land		6		7
	Agriculture Land		7		9
Lineament Density	Very High	7	7	2	9
	High		6		7
	Medium		5		5
	Low		4		3
	Very Low		3		1

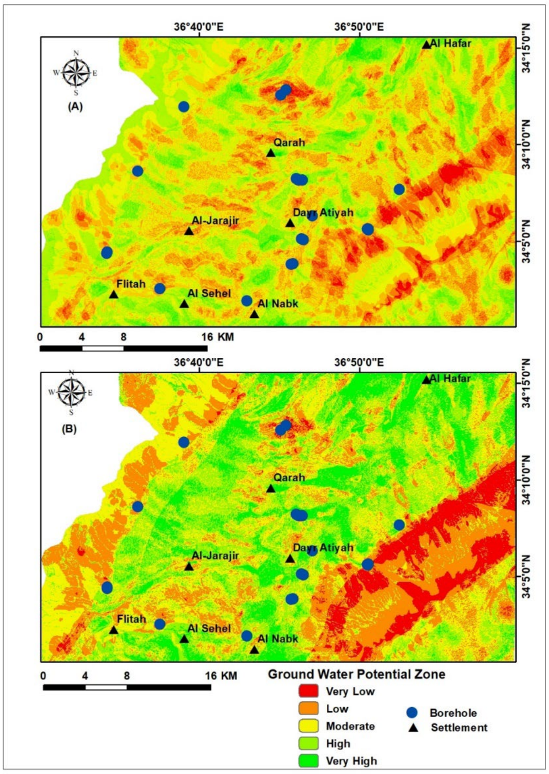

Figure A1. Groundwater Potential Zone of the (**A**) AHP1 and (**B**) MIF1 maps.

Table A2. Weight and scores of specific characteristics in (MIF2 and AHP2) are assigned to factors that influence GWPZ.

Factors	Sub-Classes	MIF2		AHP2	
		Weight	Score	Weight	Rank
Lithology	Quaternary sands, loams		20		9
	Quaternary conglomerates, sandstones, loams		16		7
	Cretaceous limestone, marl dolomites		12		5
	Neogene limestone, conglomerates, sands	20	8	31	3
	Paleogene Chalky limestone, marls		4		1
Slope	80–87		2		1
	60–80		6		3
	40–60		10		5
	20–40	18	14	21	7
	0–20		18		9
Drainage Density	Very Low		15		9
	Low		12		7
	Medium		9		5
	High	15	6	16	3
	Very High		3		1
Geomorphology	Flood plain		13		9
	Upper quaternary and recent alluvial fans		10		7
	Low mountains with small and low ridges		7		5
	Desert weathering outliers		4		3
	Low mountains with coniform and cuesta- hilly relief		1		1
	Medium-height mountains with flattened divides and steep abrupt slopes	13	1	11	1
LULC	Built-Up Land		3		1
	Bare Mountain		5		3
	Barren Land		7		5
	Pasture Land	11	9	9	7
	Agriculture Land		11		9
Lineament Density	Very Low		1		1
	Low		3		3
	Medium		5		5
	High	9	7	5	7
	Very High		9		9
Rainfall (mm)	270–430		7		9
	197–270		6		7
	163–197		5		5
	139–163	7	4	4	3
	111–139		3		1
Soil	Entisols-Lithic Torriorthents, Coarse and medium-Orthids, level to Steep.		7		9
	Entisols-Lithic Torriorthents, Coarse and medium-Rock outcrop, steep.		6		7
	Aridisols-Typic Camborthids, medium- Typic Calciorthids, Level.		5		5
	Aridisols-Typic Paleorthids, Coarse and medium-level sloping and steep.	7	4	3	3
	Aridisols-Typic Calciorthids, Coarse- Paleorthids, Sloping.		3		

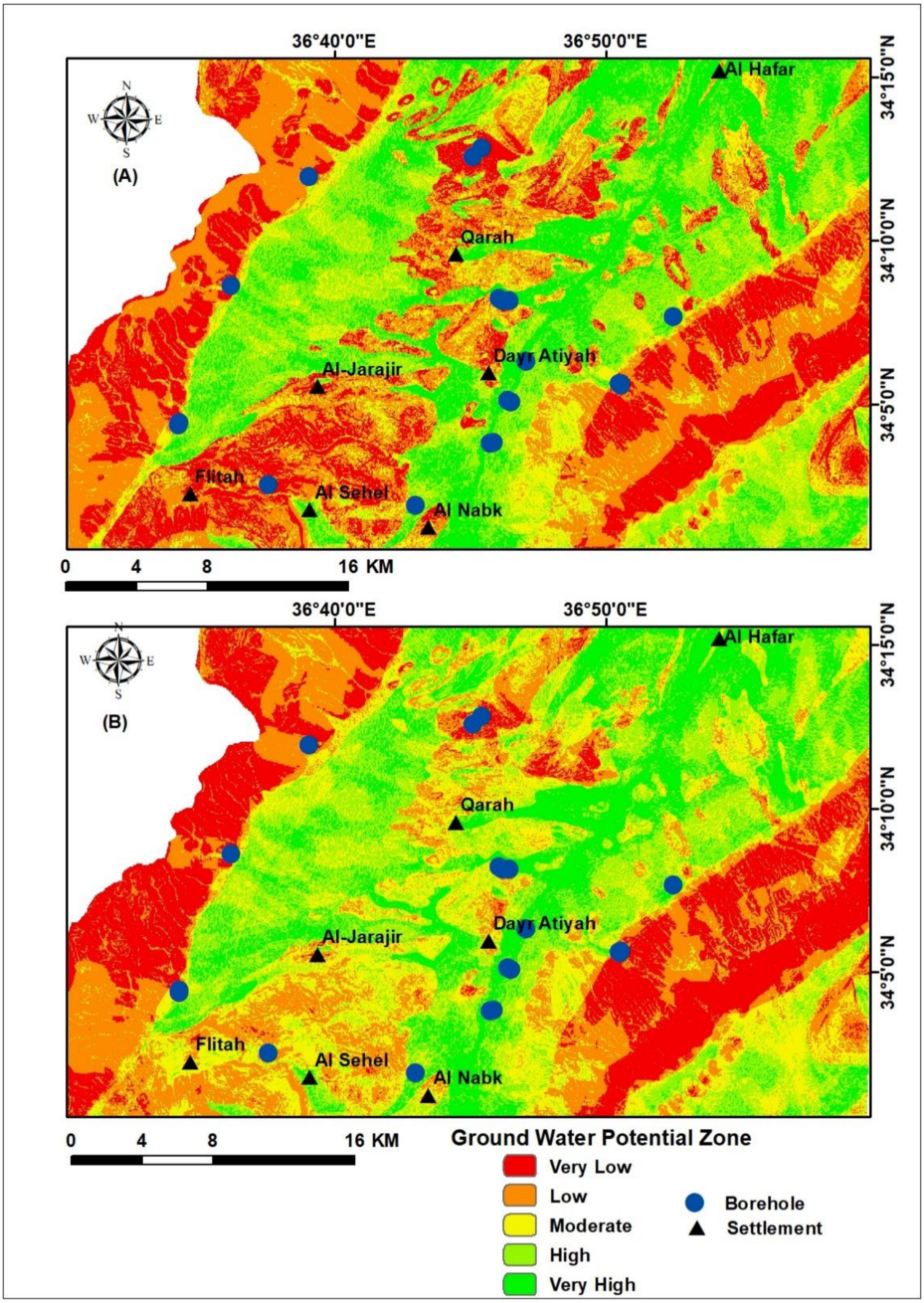

Figure A2. Groundwater Potential Zone of the (**A**) AHP2 and (**B**) MIF2 maps.

Table A3. Weight and scores of specific characteristics in (MIF3 and AHP3) are assigned to factors that influence GWPZ.

Factors	Sub-Classes	MIF3		AHP3	
		Weight	Score	Weight	Rank
Lithology	Quaternary sands, loams	20	20	31	9
	Quaternary conglomerates, sandstones, loams		16		7
	Cretaceous limestone, marl dolomites		12		5
	Neogene limestone, conglomerates, sands		8		3
	Paleogene Chalky limestone, marls		4		1
Slope	80–87	18	2	22	1
	60–80		6		3
	40–60		10		5
	20–40		14		7
	0–20		18		9
Geomorphology	Flood plain	15	15	16	9
	Upper quaternary and recent alluvial fans		12		7
	Low mountains with small and low ridges		9		5
	Desert weathering outliers		6		3
	Low mountains with coniform and cuesta- hilly relief		3		1
	Medium-height mountains with flattened divides and steep abrupt slopes		1		1
Drainage Density	Very Low	13	13	11	9
	Low		10		7
	Medium		7		5
	High		4		3
	Very High		1		1
LULC	Built-Up Land	11	3	9	1
	Bare Mountain		5		3
	Barren Land		7		5
	Pasture Land		9		7
	Agriculture Land		11		9
Lineament Density	Very Low	9	1	5	1
	Low		3		3
	Medium		5		5
	High		7		7
	Very High		9		9
Rainfall (mm)	270–430	7	7	4	9
	197–270		6		7
	163–197		5		5
	139–163		4		3
	111–139		3		1
Soil	Entisols-Lithic Torriorthents, Coarse and medium-Orthids, level to Steep.	7	7	2	9
	Entisols-Lithic Torriorthents, Coarse and medium-Rock outcrop, steep.		6		7
	Aridisols-Typic Camborthids, medium-Typic Calciorthids, Level.		5		5
	Aridisols-Typic Paleorthids, Coarse and medium-level sloping and steep.		4		3
	Aridisols-Typic Calciorthids, Coarse-Paleorthids, Sloping.		3		1

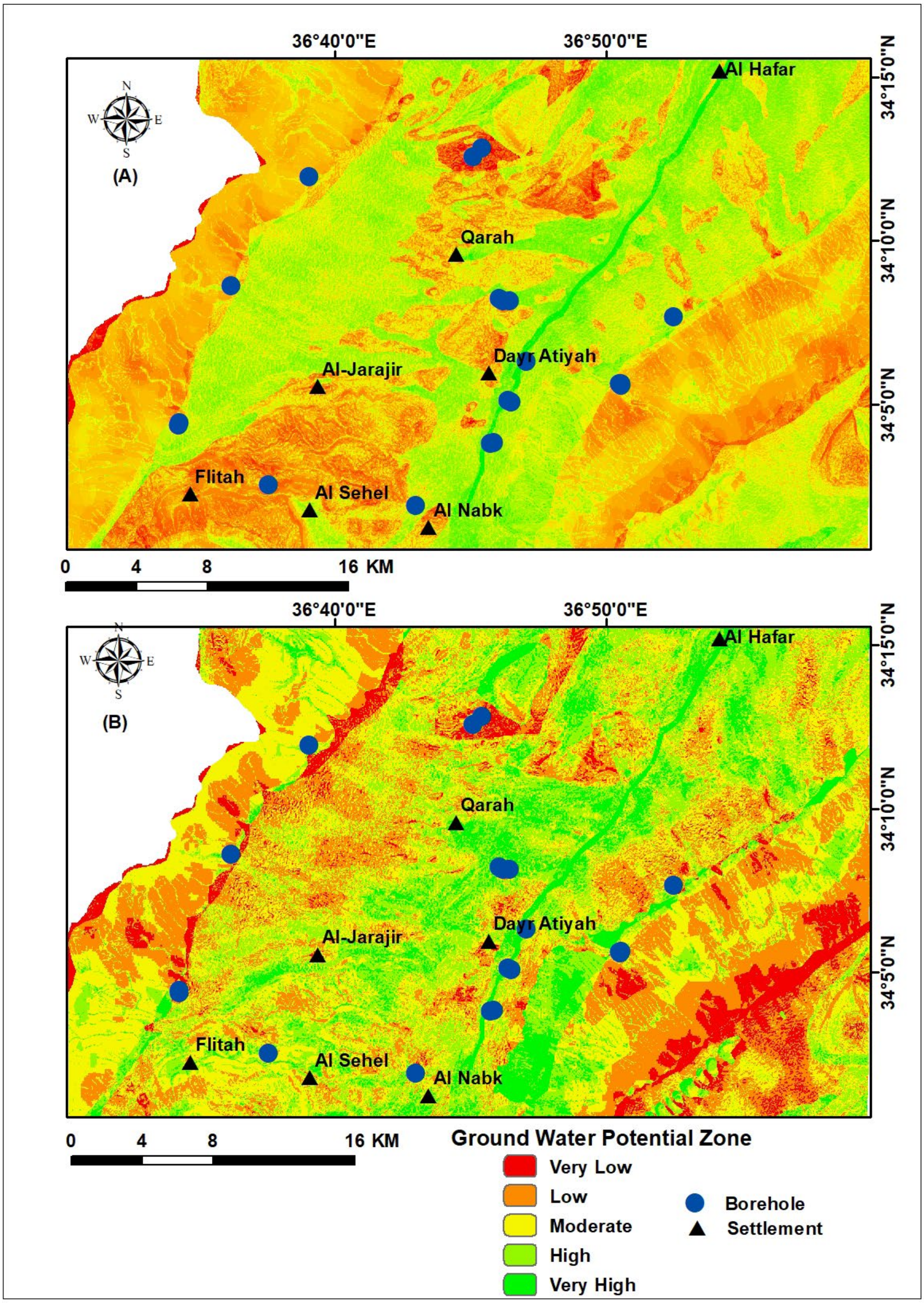

Figure A3. Groundwater Potential Zone of the (**A**) AHP3 and (**B**) MIF3 maps.

Table A4. Weight and scores of specific characteristics in (MIF4 and AHP4) are assigned to factors that influence GWPZ.

Factors	Sub-Classes	MIF4		AHP4	
		Weight	Score	Weight	Rank
Lithology	Quaternary sands, loams	20	20	32	9
	Quaternary conglomerates, sandstones, loams		16		7
	Cretaceous limestone, marl dolomites		12		5
	Neogene limestone, conglomerates, sands		8		3
	Paleogene Chalky limestone, marls		4		1
Geomorphology	Flood plain	18	18	22	9
	Upper quaternary and recent alluvial fans		14		7
	Low mountains with small and low ridges		10		5
	Desert weathering outliers		6		3
	Low mountains with coniform and cuesta-hilly relief		2		1
	Medium-height mountains with flattened divides and steep abrupt slopes		1		1
Slope	80–87	15	3	15	1
	60–80		6		3
	40–60		9		5
	20–40		12		7
	0–20		15		9
LULC	Built-Up Land	13	1	11	1
	Bare Mountain		4		3
	Barren Land		7		5
	Pasture Land		10		7
	Agriculture Land		13		9
Drainage Density	Very Low	11	11	9	9
	Low		9		7
	Medium		7		5
	High		5		3
	Very High		3		1
Lineament Density	Very Low	9	1	5	1
	Low		3		3
	Medium		5		5
	High		7		7
	Very High		9		9
Rainfall (mm)	270–430	7	7	4	9
	197–270		6		7
	163–197		5		5
	139–163		4		3
	111–139		3		1
Soil	Entisols-Lithic Torriorthents, Coarse and medium-Orthids, level to Steep.	7	7	2	9
	Entisols-Lithic Torriorthents, Coarse and medium- Rock outcrop, steep.		6		7
	Aridisols-Typic Camborthids, medium- Typic Calciorthids, Level.		5		5
	Aridisols-Typic Paleorthids, Coarse and medium-level sloping and steep.		4		3
	Aridisols-Typic Calciorthids, Coarse- Paleorthids, Sloping.		3		1

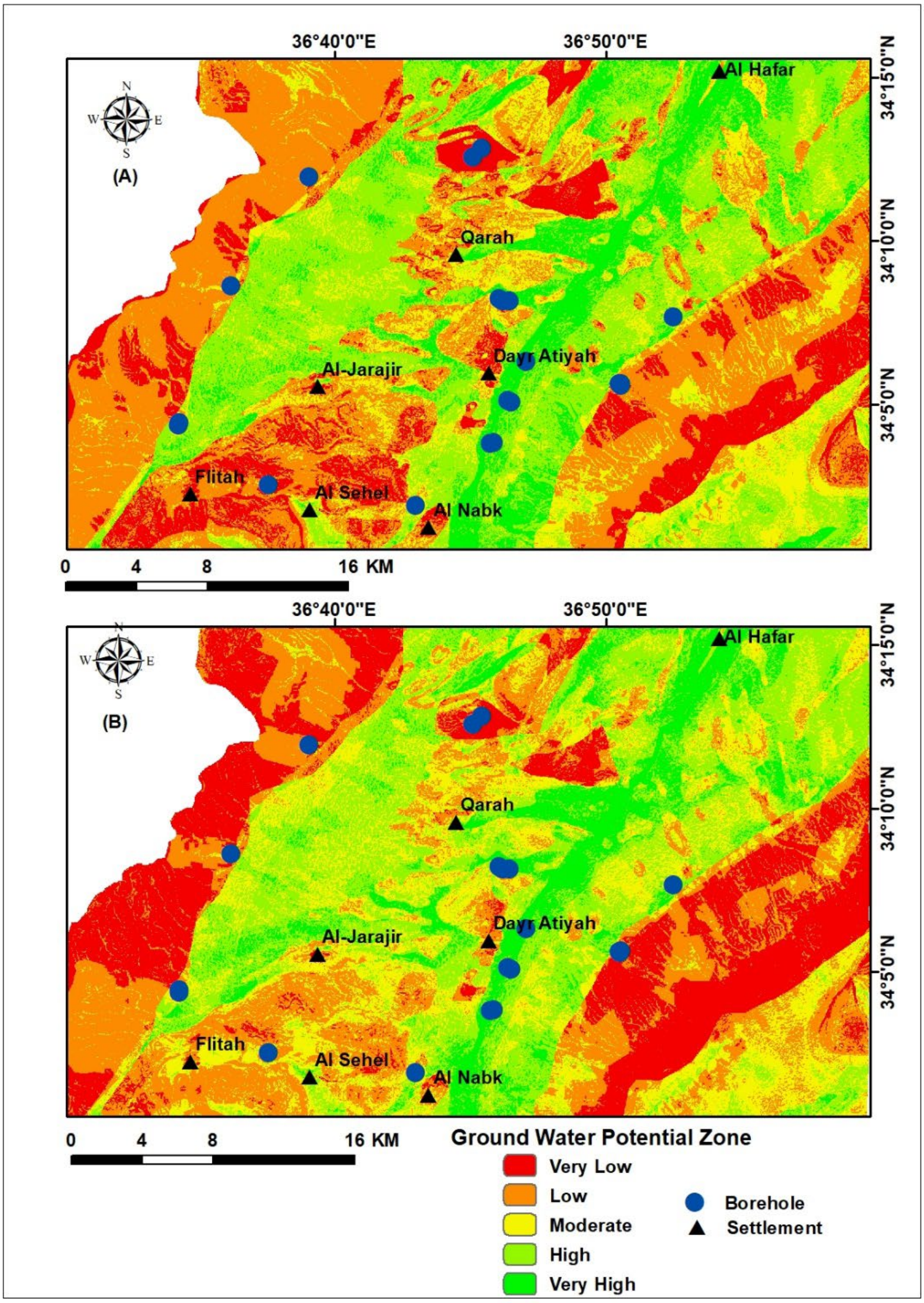

Figure A4. Groundwater Potential Zone of the (**A**) AHP4 and (**B**) MIF4 maps.

Table A5. Weight and scores of specific characteristics in (MIF5 and AHP5) are assigned to factors that influence GWPZ.

Factors	Sub-Classes	MIF5		AHP5	
		Weight	Score	Weight	Rank
Lithology	Quaternary sands, loams	20	20	32	9
	Quaternary conglomerates, sandstones, loams		16		7
	Cretaceous limestone, marl dolomites		12		5
	Neogene limestone, conglomerates, sands		8		3
	Paleogene Chalky limestone, marls		4		1
LULC	Built-Up Land	18	2	22	1
	Bare Mountain		6		3
	Barren Land		10		5
	Pasture Land		14		7
	Agriculture Land		18		9
Rainfall (mm)	270–430	15	15	15	9
	197–270		12		7
	163–197		9		5
	139–163		6		3
	111–139		3		1
Soil	Entisols-Lithic Torriorthents, Coarse and medium-Orthids, level to Steep.	13	13	11	9
	Entisols-Lithic Torriorthents, Coarse and medium-Rock outcrop, steep.		10		7
	Aridisols-Typic Camborthids, medium-Typic Calciorthids, Level		7		5
	Aridisols-Typic Paleorthids, Coarse and medium-level sloping and steep.		4		3
	Aridisols-Typic Calciorthids, Coarse-Paleorthids, Sloping.		1		1
Geomorphology	Flood plain	11	11	9	9
	Upper quaternary and recent alluvial fans		9		7
	Low mountains with small and low ridges		7		5
	Desert weathering outliers		5		3
	Low mountains with coniform and cuesta-hilly relief		3		1
	Medium-height mountains with flattened divides and steep abrupt slopes		1		1
Slope	80–87	9	1	5	1
	60–80		3		3
	40–60		5		5
	20–40		7		7
	0–20		9		9
Drainage Density	Very Low	7	7	4	9
	Low		6		7
	Medium		5		5
	High		4		3
	Very High		3		1
Lineament Density	Very Low	7	3	2	1
	Low		4		3
	Medium		5		5
	High		6		7
	Very High		7		9

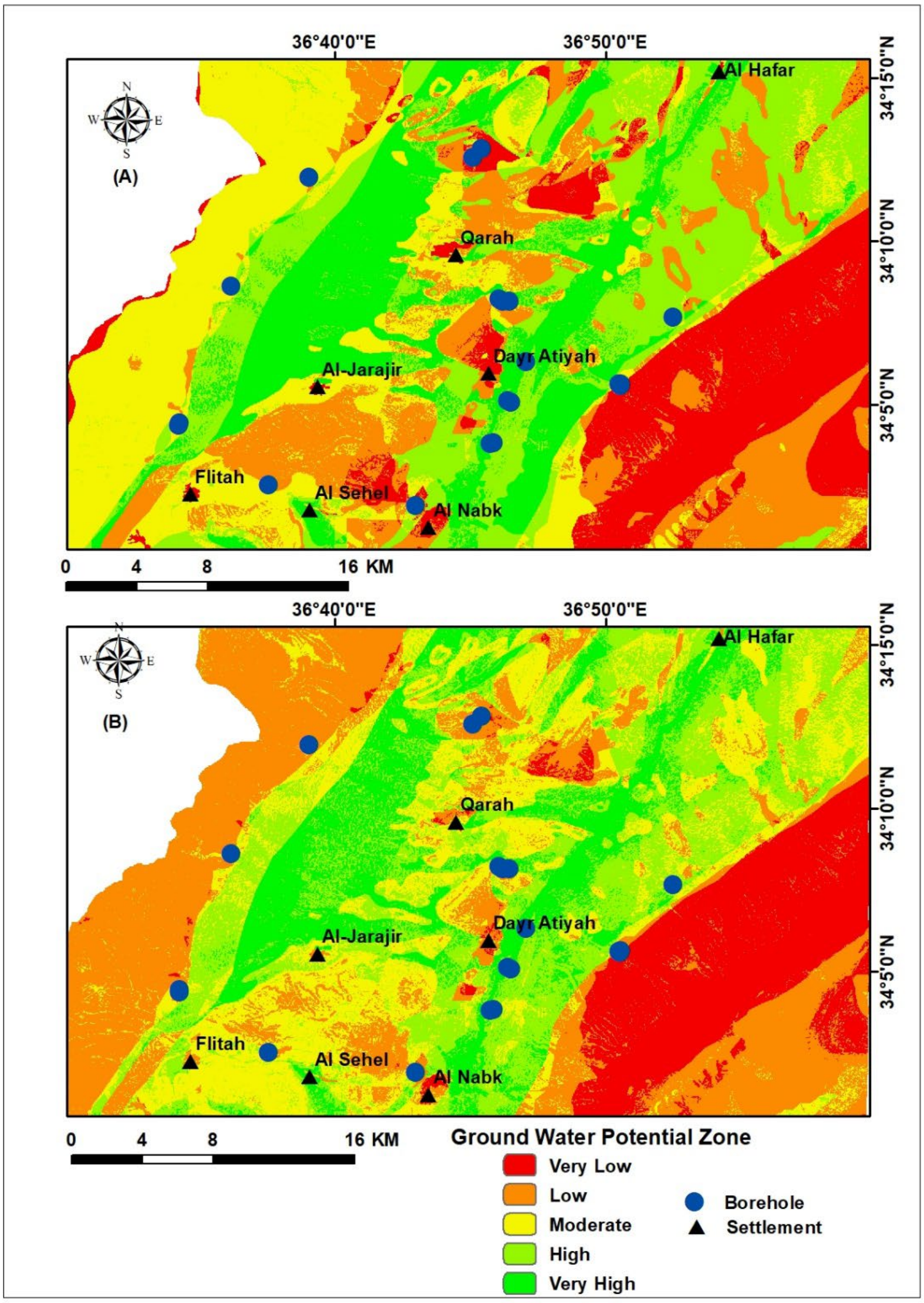

Figure A5. Groundwater Potential Zone of the (**A**) AHP5 and (**B**) MIF5 maps.

References

1. Ghorbani Nejad, S.; Falah, F.; Daneshfar, M.; Haghizadeh, A.; Rahmati, O. Delineation of Groundwater Potential Zones Using Remote Sensing and GIS-Based Data-Driven Models. *Geocarto Int.* **2017**, *32*, 167–187. [CrossRef]
2. Abd Manap, M.; Nampak, H.; Pradhan, B.; Lee, S.; Sulaiman, W.N.A.; Ramli, M.F. Application of Probabilistic-Based Frequency Ratio Model in Groundwater Potential Mapping Using Remote Sensing Data and GIS. *Arab. J. Geosci.* **2014**, *7*, 711–724. [CrossRef]
3. Rudra, K. Interrelationship between Surface and Groundwater: The Case of West Bengal. In *Ground Water Development-Issues and Sustainable Solutions*; Springer: Berlin/Heidelberg, Germany, 2019; pp. 175–181.
4. Mukherjee, P.; Singh, C.K.; Mukherjee, S. Delineation of Groundwater Potential Zones in Arid Region of India—A Remote Sensing and GIS Approach. *Water Resour. Manag.* **2012**, *26*, 2643–2672. [CrossRef]
5. Pal, S.; Kundu, S.; Mahato, S. Groundwater Potential Zones for Sustainable Management Plans in a River Basin of India and Bangladesh. *J. Clean. Prod.* **2020**, *257*, 120311. [CrossRef]

6. Pande, C.B.; Moharir, K.N.; Panneerselvam, B.; Singh, S.K.; Elbeltagi, A.; Pham, Q.B.; Varade, A.M.; Rajesh, J. Delineation of Groundwater Potential Zones for Sustainable Development and Planning Using Analytical Hierarchy Process (AHP), and MIF Techniques. *Appl. Water Sci.* **2021**, *11*, 186. [CrossRef]
7. Mallick, J.; Talukdar, S.; Kahla, N.B.; Ahmed, M.; Alsubih, M.; Almesfer, M.K.; Islam, A.R.M. A Novel Hybrid Model for Developing Groundwater Potentiality Model Using High Resolution Digital Elevation Model (DEM) Derived Factors. *Water* **2021**, *13*, 2632. [CrossRef]
8. Mitra, R.; Roy, D. Delineation of Groundwater Potential Zones through the Integration of Remote Sensing, Geographic Information System, and Multi-Criteria Decision-Making Technique in the Sub-Himalayan Foothills Region, India. *Int. J. Energy Water Resour.* **2022**, 1–21. [CrossRef]
9. Karimi-Rizvandi, S.; Goodarzi, H.V.; Afkoueieh, J.H.; Chung, I.-M.; Kisi, O.; Kim, S.; Linh, N.T.T. Groundwater-Potential Mapping Using a Self-Learning Bayesian Network Model: A Comparison among Metaheuristic Algorithms. *Water* **2021**, *13*, 658. [CrossRef]
10. Elmahdy, S.; Ali, T.; Mohamed, M. Regional Mapping of Groundwater Potential in Ar Rub Al Khali, Arabian Peninsula Using the Classification and Regression Trees Model. *Remote Sens.* **2021**, *13*, 2300. [CrossRef]
11. Magesh, N.S.; Chandrasekar, N.; Soundranayagam, J.P. Delineation of Groundwater Potential Zones in Theni District, Tamil Nadu, Using Remote Sensing, GIS and MIF Techniques. *Geosci. Front.* **2012**, *3*, 189–196. [CrossRef]
12. Ghayoumian, J.; Saravi, M.M.; Feiznia, S.; Nouri, B.; Malekian, A. Application of GIS Techniques to Determine Areas Most Suitable for Artificial Groundwater Recharge in a Coastal Aquifer in Southern Iran. *J. Asian Earth Sci.* **2007**, *30*, 364–374. [CrossRef]
13. Jha, M.K.; Chowdhury, A.; Chowdary, V.M.; Peiffer, S. Groundwater Management and Development by Integrated Remote Sensing and Geographic Information Systems: Prospects and Constraints. *Water Resour. Manag.* **2007**, *21*, 427–467. [CrossRef]
14. Prasad, R.K.; Mondal, N.C.; Banerjee, P.; Nandakumar, M.V.; Singh, V.S. Deciphering Potential Groundwater Zone in Hard Rock through the Application of GIS. *Environ. Geol.* **2008**, *55*, 467–475. [CrossRef]
15. Chowdhury, A.; Jha, M.K.; Chowdary, V.M.; Mal, B.C. Integrated Remote Sensing and GIS-based Approach for Assessing Groundwater Potential in West Medinipur District, West Bengal, India. *Int. J. Remote Sens.* **2009**, *30*, 231–250. [CrossRef]
16. Saha, D.; Dhar, Y.R.; Vittala, S.S. Delineation of Groundwater Development Potential Zones in Parts of Marginal Ganga Alluvial Plain in South Bihar, Eastern India. *Environ. Monit. Assess.* **2010**, *165*, 179–191. [CrossRef]
17. Machiwal, D.; Jha, M.K.; Mal, B.C. Assessment of Groundwater Potential in a Semi-Arid Region of India Using Remote Sensing, GIS and MCDM Techniques. *Water Resour. Manag.* **2011**, *25*, 1359–1386. [CrossRef]
18. Teixeira, J.; Chaminé, H.I.; Carvalho, J.M.; Pérez-Alberti, A.; Rocha, F. Hydrogeomorphological Mapping as a Tool in Groundwater Exploration. *J. Maps* **2013**, *9*, 263–273. [CrossRef]
19. Teixeira, J.; Chaminé, H.I.; Marques, J.E.; Carvalho, J.M.; Pereira, A.; Carvalho, M.R.; Fonseca, P.E.; Pérez-Alberti, A.; Rocha, F. A Comprehensive Analysis of Groundwater Resources Using GIS and Multicriteria Tools (Caldas Da Cavaca, Central Portugal): Environmental Issues. *Environ. Earth Sci.* **2015**, *73*, 2699–2715. [CrossRef]
20. Jasrotia, A.S.; Kumar, A.; Singh, R. Integrated Remote Sensing and GIS Approach for Delineation of Groundwater Potential Zones Using Aquifer Parameters in Devak and Rui Watershed of Jammu and Kashmir, India. *Arab. J. Geosci.* **2016**, *9*, 304. [CrossRef]
21. Abijith, D.; Saravanan, S.; Singh, L.; Jennifer, J.J.; Saranya, T.; Parthasarathy, K.S.S. GIS-Based Multi-Criteria Analysis for Identification of Potential Groundwater Recharge Zones-a Case Study from Ponnaniyaru Watershed, Tamil Nadu, India. *HydroResearch* **2020**, *3*, 1–14. [CrossRef]
22. Bhattacharya, S.; Das, S.; Das, S.; Kalashetty, M.; Warghat, S.R. An Integrated Approach for Mapping Groundwater Potential Applying Geospatial and MIF Techniques in the Semiarid Region. *Environ. Dev. Sustain.* **2021**, *23*, 495–510. [CrossRef]
23. Nag, S.K.; Chowdhury, P. Decipherment of Potential Zones for Groundwater Occurrence: A Study in Khatra Block, Bankura District, West Bengal, Using Geospatial Techniques. *Environ. Earth Sci.* **2019**, *78*, 49. [CrossRef]
24. Wind, Y.; Saaty, T.L. Marketing Applications of the Analytic Hierarchy Process. *Manag. Sci.* **1980**, *26*, 641–658. [CrossRef]
25. Salar, S.G.; Othman, A.A.; Hasan, S.E. Identification of Suitable Sites for Groundwater Recharge in Awaspi Watershed Using GIS and Remote Sensing Techniques. *Environ. Earth Sci.* **2018**, *77*, 701. [CrossRef]
26. Al-Ruzouq, R.; Shanableh, A.; Merabtene, T.; Siddique, M.; Khalil, M.A.; Idris, A.; Almulla, E. Potential Groundwater Zone Mapping Based on Geo-Hydrological Considerations and Multi-Criteria Spatial Analysis: North UAE. *Catena* **2019**, *173*, 511–524. [CrossRef]
27. Thapa, R.; Gupta, S.; Guin, S.; Kaur, H. Assessment of Groundwater Potential Zones Using Multi-Influencing Factor (MIF) and GIS: A Case Study from Birbhum District, West Bengal. *Appl. Water Sci.* **2017**, *7*, 4117–4131. [CrossRef]
28. Othman, A.A.; Obaid, A.K.; Al-Manmi, D.A.M.; Pirouei, M.; Salar, S.G.; Liesenberg, V.; Al-Maamar, A.F.; Shihab, A.T.; Al-Saady, Y.I.; Al-Attar, Z.T. Insights for Landfill Site Selection Using Gis: A Case Study in the Tanjero River Basin, Kurdistan Region, Iraq. *Sustainability* **2021**, *13*, 12602. [CrossRef]
29. Bashir, B.; Alsalman, A.; Othman, A.A.; Obaid, A.K.; Bashir, H. New Approach to Selecting Civil Defense Centers in Al-Riyadh City (Ksa) Based on Multi-Criteria Decision Analysis and Gis. *Land* **2021**, *10*, 1108. [CrossRef]
30. Othman, A.A.; Al- Maamar, A.F.; Al-Manmi, D.A.M.; Veraldo, L.; Hasan, S.E.; Obaid, A.K.; Al-Quraishi, A.M.F. GIS-Based Modeling for Selection of Dam Sites in the Kurdistan Region, Iraq. *ISPRS Int. J. Geo.-Inf.* **2020**, *9*, 244. [CrossRef]
31. Agarwal, R.; Garg, P.K. Remote Sensing and GIS Based Groundwater Potential & Recharge Zones Mapping Using Multi-Criteria Decision Making Technique. *Water Resour. Manag.* **2016**, *30*, 243–260.

32. Singh, L.K.; Jha, M.K.; Chowdary, V.M. Assessing the Accuracy of GIS-Based Multi-Criteria Decision Analysis Approaches for Mapping Groundwater Potential. *Ecol. Indic.* **2018**, *91*, 24–37. [CrossRef]
33. Shekhar, S.; Pandey, A.C. Delineation of Groundwater Potential Zone in Hard Rock Terrain of India Using Remote Sensing, Geographical Information System (GIS) and Analytic Hierarchy Process (AHP) Techniques. *Geocarto Int.* **2015**, *30*, 402–421. [CrossRef]
34. Murmu, P.; Kumar, M.; Lal, D.; Sonker, I.; Singh, S.K. Delineation of Groundwater Potential Zones Using Geospatial Techniques and Analytical Hierarchy Process in Dumka District, Jharkhand, India. *Groundw. Sustain. Dev.* **2019**, *9*, 100239. [CrossRef]
35. Dey, S.; Shukla, U.K.; Mehrishi, P.; Mall, R.K. Appraisal of Groundwater Potentiality of Multilayer Alluvial Aquifers of the Varuna River Basin, India, Using Two Concurrent Methods of MCDM. *Environ. Dev. Sustain.* **2021**, *23*, 17558–17589. [CrossRef]
36. Taheri, K.; Missimer, T.M.; Taheri, M.; Moayedi, H.; Mohseni Pour, F. Critical Zone Assessments of an Alluvial Aquifer System Using the Multi-Influencing Factor (MIF) and Analytical Hierarchy Process (AHP) Models in Western Iran. *Nat. Resour. Res.* **2020**, *29*, 1163–1191. [CrossRef]
37. Sutradhar, S.; Mondal, P.; Das, N. Delineation of Groundwater Potential Zones Using MIF and AHP Models: A Micro-Level Study on Suri Sadar Sub-Division, Birbhum District, West Bengal, India. *Groundw. Sustain. Dev.* **2021**, *12*, 100547. [CrossRef]
38. Zghibi, A.; Mirchi, A.; Msaddek, M.H.; Merzougui, A.; Zouhri, L.; Taupin, J.-D.; Chekirbane, A.; Chenini, I.; Tarhouni, J. Using Analytical Hierarchy Process and Multi-Influencing Factors to Map Groundwater Recharge Zones in a Semi-Arid Mediterranean Coastal Aquifer. *Water* **2020**, *12*, 2525. [CrossRef]
39. Abrams, W.; Ghoneim, E.; Shew, R.; LaMaskin, T.; Al-Bloushi, K.; Hussein, S.; AbuBakr, M.; Al-Mulla, E.; Al-Awar, M.; El-Baz, F. Delineation of Groundwater Potential (GWP) in the Northern United Arab Emirates and Oman Using Geospatial Technologies in Conjunction with Simple Additive Weight (SAW), Analytical Hierarchy Process (AHP), and Probabilistic Frequency Ratio (PFR) Techniques. *J. Arid Environ.* **2018**, *157*, 77–96. [CrossRef]
40. Das, B.; Pal, S.C. Combination of GIS and Fuzzy-AHP for Delineating Groundwater Recharge Potential Zones in the Critical Goghat-II Block of West Bengal, India. *HydroResearch* **2019**, *2*, 21–30. [CrossRef]
41. Elewa, H.H.; Qaddah, A.A. Groundwater Potentiality Mapping in the Sinai Peninsula, Egypt, Using Remote Sensing and GIS-Watershed-Based Modeling. *Hydrogeol. J.* **2011**, *19*, 613–628. [CrossRef]
42. Yeh, H.-F.; Lee, C.-H.; Hsu, K.-C.; Chang, P.-H. GIS for the Assessment of the Groundwater Recharge Potential Zone. *Environ. Geol.* **2009**, *58*, 185–195. [CrossRef]
43. Das, S. Comparison among Influencing Factor, Frequency Ratio, and Analytical Hierarchy Process Techniques for Groundwater Potential Zonation in Vaitarna Basin, Maharashtra, India. *Groundw. Sustain. Dev.* **2019**, *8*, 617–629. [CrossRef]
44. Ahmed, A.; Ranasinghe-Arachchilage, C.; Alrajhi, A.; Hewa, G. Comparison of Multicriteria Decision-Making Techniques for Groundwater Recharge Potential Zonation: Case Study of the Willochra Basin, South Australia. *Water* **2021**, *13*, 525. [CrossRef]
45. Bera, A.; Mukhopadhyay, B.P.; Barua, S. Delineation of Groundwater Potential Zones in Karha River Basin, Maharashtra, India, Using AHP and Geospatial Techniques. *Arab. J. Geosci.* **2020**, *13*, 693. [CrossRef]
46. Pathmanandakumar, V.; Thasarathan, N.; Ranagalage, M. An Approach to Delineate Potential Groundwater Zones in Kilinochchi District, Sri Lanka, Using GIS Techniques. *ISPRS Int. J. Geo.-Inf.* **2021**, *10*, 730. [CrossRef]
47. Dar, T.; Rai, N.; Bhat, A. Delineation of Potential Groundwater Recharge Zones Using Analytical Hierarchy Process (AHP). *Geol. Ecol. Landsc.* **2021**, *5*, 292–307. [CrossRef]
48. Koirala, P.; Thakuri, S.; Joshi, S.; Chauhan, R. Estimation of Soil Erosion in Nepal Using a RUSLE Modeling and Geospatial Tool. *Geosciences* **2019**, *9*, 147. [CrossRef]
49. Kanagaraj, G.; Suganthi, S.; Elango, L.; Magesh, N.S. Assessment of Groundwater Potential Zones in Vellore District, Tamil Nadu, India Using Geospatial Techniques. *Earth Sci. Inform.* **2019**, *12*, 211–223. [CrossRef]
50. Etikala, B.; Golla, V.; Li, P.; Renati, S. Deciphering Groundwater Potential Zones Using MIF Technique and GIS: A Study from Tirupati Area, Chittoor District, Andhra Pradesh, India. *HydroResearch* **2019**, *1*, 1–7. [CrossRef]
51. Arulbalaji, P.; Padmalal, D.; Sreelash, K. GIS and AHP Techniques Based Delineation of Groundwater Potential Zones: A Case Study from Southern Western Ghats, India. *Sci. Rep.* **2019**, *9*, 2082. [CrossRef]
52. Onur, T.; Gök, R.; Abdulnaby, W.; Mahdi, H.; Numan, N.M.S.; Al-Shukri, H.; Shakir, A.M.; Chlaib, H.K.; Ameen, T.H.; Abd, N.A. A Comprehensive Earthquake Catalog for Iraq in Terms of Moment Magnitude. *Seismol. Res. Lett.* **2017**, *88*, 798–811. [CrossRef]
53. Lakshmi, S.V.; Reddy, Y.V.K. Identification of Groundwater Potential Zones Using GIS and Remote Sensing. *Int. J. Pure Appl. Math.* **2018**, *119*, 3195–3210.
54. Hussein, A.-A.; Govindu, V.; Nigusse, A.G.M. Evaluation of Groundwater Potential Using Geospatial Techniques. *Appl. Water Sci.* **2017**, *7*, 2447–2461. [CrossRef]
55. Ajay Kumar, V.; Mondal, N.C.; Ahmed, S. Identification of Groundwater Potential Zones Using RS, GIS and AHP Techniques: A Case Study in a Part of Deccan Volcanic Province (DVP), Maharashtra, India. *J. Indian Soc. Remote Sens.* **2020**, *48*, 497–511. [CrossRef]
56. Senapati, U.; Das, T.K. GIS-Based Comparative Assessment of Groundwater Potential Zone Using MIF and AHP Techniques in Cooch Behar District, West Bengal. *Appl. Water Sci.* **2022**, *12*, 43. [CrossRef]
57. Goswami, T.; Ghosal, S. Understanding the Suitability of Two MCDM Techniques in Mapping the Groundwater Potential Zones of Semi-Arid Bankura District in Eastern India. *Groundw. Sustain. Dev.* **2022**, *17*, 100727. [CrossRef]

58. Allafta, H.; Opp, C.; Patra, S. Identification of Groundwater Potential Zones Using Remote Sensing and GIS Techniques: A Case Study of the Shatt Al-Arab Basin. *Remote Sens.* **2020**, *13*, 112. [CrossRef]
59. Kolli, M.K.; Opp, C.; Groll, M. Mapping of Potential Groundwater Recharge Zones in the Kolleru Lake Catchment, India, by Using Remote Sensing and GIS Techniques. *Nat. Resour.* **2020**, *11*, 127. [CrossRef]
60. Benjmel, K.; Amraoui, F.; Boutaleb, S.; Ouchchen, M.; Tahiri, A.; Touab, A. Mapping of Groundwater Potential Zones in Crystalline Terrain Using Remote Sensing, GIS Techniques, and Multicriteria Data Analysis (Case of the Ighrem Region, Western Anti-Atlas, Morocco). *Water* **2020**, *12*, 471. [CrossRef]
61. Arshad, A.; Zhang, Z.; Zhang, W.; Dilawar, A. Mapping Favorable Groundwater Potential Recharge Zones Using a GIS-Based Analytical Hierarchical Process and Probability Frequency Ratio Model: A Case Study from an Agro-Urban Region of Pakistan. *Geosci. Front.* **2020**, *11*, 1805–1819. [CrossRef]
62. Choubin, B.; Rahmati, O.; Soleimani, F.; Alilou, H.; Moradi, E.; Alamdari, N. Regional Groundwater Potential Analysis Using Classification and Regression Trees. In *Spatial Modeling in GIS and R for Earth and Environmental Sciences*; Elsevier: Amsterdam, The Netherlands, 2019; pp. 485–498.
63. Patra, S.; Mishra, P.; Mahapatra, S.C. Delineation of Groundwater Potential Zone for Sustainable Development: A Case Study from Ganga Alluvial Plain Covering Hooghly District of India Using Remote Sensing, Geographic Information System and Analytic Hierarchy Process. *J. Clean. Prod.* **2018**, *172*, 2485–2502. [CrossRef]
64. Nasir, M.J.; Khan, S.; Zahid, H.; Khan, A. Delineation of Groundwater Potential Zones Using GIS and Multi Influence Factor (MIF) Techniques: A Study of District Swat, Khyber Pakhtunkhwa, Pakistan. *Environ. Earth Sci.* **2018**, *77*, 367. [CrossRef]
65. The General Company for Water Studies. The Qalamoun Water Study Project, Volume Three, Hydrogeological Report. Homs, 1994.
66. Ponikarov, V.P.; Kozlov, V.V.; Artemove, A.V.; Kalis, A.F. *The Geology of Syria. Explanatory Notes on the Geological Map of Syria, Scale 1:200,000*; Syrian Arab Republic, Ministry of Industry, Departement of Geological and Mineral Research: Damascus, Syria, 1966.
67. Mohammed, S.; Khallouf, A.; Kiwan, S.; Alhenawi, S.; Ali, H.; Harsányi, E. Characterization of Major Soil Orders in Syria 1. *Eurasian Soil Sci.* **2020**, *53*, 420–429. [CrossRef]
68. TECHNOEXPORT, M.O.G.U. *Geological Map Of Syria Scale 1:200,000, Sheets I-36-XVIII, I-37-XIII (Trablus, Homs)*; Ministry of Industry, S.A.R.: Damascus, Syria, 1963.
69. Llaiwi, M.D. *Soil Map of Syria and Lebanon Scale 1:1,000,000*; The Arab Center for the Studies of Arid Zones and Dry Lands, (ACSAD): Damascus, Syria, 1985.
70. Mirzayev, K. *Geological Map of Syria*; Syrian Arab Republic Ministry of Industry Department of Geological and Mineral Research: Damascus, Syria, 1963.
71. USGS EarthExplorer. Available online: https://earthexplorer.usgs.gov/ (accessed on 10 April 2020).
72. Dinku, T.; Funk, C.; Peterson, P.; Maidment, R.; Tadesse, T.; Gadain, H.; Ceccato, P. Validation of the CHIRPS Satellite Rainfall Estimates over Eastern Africa. *Q. J. R. Meteorol. Soc.* **2018**, *144*, 292–312. [CrossRef]
73. Bai, L.; Shi, C.; Li, L.; Yang, Y.; Wu, J. Accuracy of CHIRPS Satellite-Rainfall Products over Mainland China. *Remote Sens.* **2018**, *10*, 362. [CrossRef]
74. Saeidizand, R.; Sabetghadam, S.; Tarnavsky, E.; Pierleoni, A. Evaluation of CHIRPS Rainfall Estimates over Iran. *Q. J. R. Meteorol. Soc.* **2018**, *144*, 282–291. [CrossRef]
75. Sulugodu, B.; Deka, P.C. Evaluating the Performance of CHIRPS Satellite Rainfall Data for Streamflow Forecasting. *Water Resour. Manag.* **2019**, *33*, 3913–3927. [CrossRef]
76. Ocampo-Marulanda, C.; Fernández-Álvarez, C.; Cerón, W.L.; Canchala, T.; Carvajal-Escobar, Y.; Alfonso-Morales, W. A Spatiotemporal Assessment of the High-Resolution CHIRPS Rainfall Dataset in Southwestern Colombia Using Combined Principal Component Analysis. *Ain Shams Eng. J.* **2022**, *13*, 101739. [CrossRef]
77. Abdourahamane, Z.S.; Garba, I.; Boukary, A.G.; Mirzabaev, A. Spatiotemporal Characterization of Agricultural Drought in the Sahel Region Using a Composite Drought Index. *J. Arid Environ.* **2022**, *204*, 104789. [CrossRef]
78. FAO. Food and Agriculture Organization of the United Nation. Available online: https://wapor.apps.fao.org (accessed on 15 May 2020).
79. Das, S.; Pardeshi, S.D. Integration of Different Influencing Factors in GIS to Delineate Groundwater Potential Areas Using IF and FR Techniques: A Study of Pravara Basin, Maharashtra, India. *Appl. Water Sci.* **2018**, *8*, 197. [CrossRef]
80. Saaty, T.L. A Scaling Method for Priorities in Hierarchical Structures. *J. Math. Psychol.* **1977**, *15*, 234–281. [CrossRef]
81. Saaty, T.L.; Vargas, L.G. Dispersion of Group Judgments. *Math. Comput. Model.* **2007**, *46*, 918–925. [CrossRef]
82. Saaty, T.L. Fundamentals of the Analytic Network Process—Multiple Networks with Benefits, Costs, Opportunities and Risks. *J. Syst. Sci. Syst. Eng.* **2004**, *13*, 348–379. [CrossRef]
83. Saaty, T.L. Decision Making with the Analytic Hierarchy Process. *Int. J. Serv. Sci.* **2008**, *1*, 83–98. [CrossRef]
84. Thirumalaivasan, D.; Karmegam, M.; Venugopal, K. AHP-DRASTIC: Software for Specific Aquifer Vulnerability Assessment Using DRASTIC Model and GIS. *Environ. Model. Softw.* **2003**, *18*, 645–656. [CrossRef]
85. Pilevar, A.R.; Matinfar, H.R.; Sohrabi, A.; Sarmadian, F. Integrated Fuzzy, AHP and GIS Techniques for Land Suitability Assessment in Semi-Arid Regions for Wheat and Maize Farming. *Ecol. Indic.* **2020**, *110*, 105887. [CrossRef]
86. Souissi, D.; Msaddek, M.H.; Zouhri, L.; Chenini, I.; El May, M.; Dlala, M. Mapping Groundwater Recharge Potential Zones in Arid Region Using GIS and Landsat Approaches, Southeast Tunisia. *Hydrol. Sci. J.* **2018**, *63*, 251–268. [CrossRef]

87. Arya, S.; Subramani, T.; Karunanidhi, D. Delineation of Groundwater Potential Zones and Recommendation of Artificial Recharge Structures for Augmentation of Groundwater Resources in Vattamalaikarai Basin, South India. *Environ. Earth Sci.* **2020**, *79*, 102. [CrossRef]
88. Fashae, O.A.; Tijani, M.N.; Talabi, A.O.; Adedeji, O.I. Delineation of Groundwater Potential Zones in the Crystalline Basement Terrain of SW-Nigeria: An Integrated GIS and Remote Sensing Approach. *Appl. Water Sci.* **2014**, *4*, 19–38. [CrossRef]
89. Rahmati, O.; Samani, A.N.; Mahdavi, M.; Pourghasemi, H.R.; Zeinivand, H. Groundwater Potential Mapping at Kurdistan Region of Iran Using Analytic Hierarchy Process and GIS. *Arab. J. Geosci.* **2015**, *8*, 7059–7071. [CrossRef]
90. Saranya, T.; Saravanan, S. Groundwater Potential Zone Mapping Using Analytical Hierarchy Process (AHP) and GIS for Kancheepuram District, Tamilnadu, India. *Model. Earth Syst. Environ.* **2020**, *6*, 1105–1122. [CrossRef]
91. Mohammady, M.; Pourghasemi, H.R.; Pradhan, B. Landslide Susceptibility Mapping at Golestan Province, Iran: A Comparison between Frequency Ratio, Dempster–Shafer, and Weights-of-Evidence Models. *J. Asian Earth Sci.* **2012**, *61*, 221–236. [CrossRef]
92. Pradhan, B. Groundwater Potential Zonation for Basaltic Watersheds Using Satellite Remote Sensing Data and GIS Techniques. *Cent. Eur. J. Geosci.* **2009**, *1*, 120–129. [CrossRef]
93. Pourghasemi, H.R.; Moradi, H.R.; Fatemi Aghda, S.M. Landslide Susceptibility Mapping by Binary Logistic Regression, Analytical Hierarchy Process, and Statistical Index Models and Assessment of Their Performances. *Nat. Hazards* **2013**, *69*, 749–779. [CrossRef]
94. Naghibi, S.A.; Moradi Dashtpagerdi, M. Evaluation of Four Supervised Learning Methods for Groundwater Spring Potential Mapping in Khalkhal Region (Iran) Using GIS-Based Features. *Hydrogeol. J.* **2017**, *25*, 169–189. [CrossRef]
95. Pourtaghi, Z.S.; Pourghasemi, H.R. GIS-Based Groundwater Spring Potential Assessment and Mapping in the Birjand Township, Southern Khorasan Province, Iran. *Hydrogeol. J.* **2014**, *22*, 643–662. [CrossRef]
96. Nag, S.K.; Ghosh, P. Delineation of Groundwater Potential Zone in Chhatna Block, Bankura District, West Bengal, India Using Remote Sensing and GIS Techniques. *Environ. Earth Sci.* **2013**, *70*, 2115–2127. [CrossRef]
97. Senanayake, I.P.; Dissanayake, D.; Mayadunna, B.B.; Weerasekera, W.L. An Approach to Delineate Groundwater Recharge Potential Sites in Ambalantota, Sri Lanka Using GIS Techniques. *Geosci. Front.* **2016**, *7*, 115–124. [CrossRef]
98. Chitsazan, M.; Akhtari, Y. A GIS-Based DRASTIC Model for Assessing Aquifer Vulnerability in Kherran Plain, Khuzestan, Iran. *Water Resour. Manag.* **2009**, *23*, 1137–1155. [CrossRef]
99. Al-manmi, D.A.M.; Rauf, L.F. Groundwater Potential Mapping Using Remote Sensing and GIS-Based, in Halabja City, Kurdistan, Iraq. *Arab. J. Geosci.* **2016**, *9*, 357. [CrossRef]
100. Mohammed, D.A.; Mohammed, S.H.; Szűcs, P. Integrated Remote Sensing and GIS Techniques to Delineate Groundwater Potential Area of Chamchamal Basin, Sulaymaniyah, NE Iraq. *Kuwait J. Sci.* **2021**, *48*. [CrossRef]
101. Şener, E.; Şener, Ş.; Davraz, A. Groundwater Potential Mapping by Combining Fuzzy-Analytic Hierarchy Process and GIS in Beyşehir Lake Basin, Turkey. *Arab. J. Geosci.* **2018**, *11*, 187. [CrossRef]
102. Pradhan, B.; Youssef, A.M. Manifestation of Remote Sensing Data and GIS on Landslide Hazard Analysis Using Spatial-Based Statistical Models. *Arab. J. Geosci.* **2010**, *3*, 319–326. [CrossRef]
103. Pradhan, B.; Singh, R.P.; Buchroithner, M.F. Estimation of Stress and Its Use in Evaluation of Landslide Prone Regions Using Remote Sensing Data. *Adv. Sp. Res.* **2006**, *37*, 698–709. [CrossRef]
104. Subba Rao, N.; Chakradhar, G.K.J.; Srinivas, V. Identification of Groundwater Potential Zones Using Remote Sensing Techniques in and around Guntur Town, Andhra Pradesh, India. *J. Indian Soc. Remote Sens.* **2001**, *29*, 69–78. [CrossRef]
105. Chung, C.-J.F.; Fabbri, A.G. Validation of Spatial Prediction Models for Landslide Hazard Mapping. *Nat. Hazards* **2003**, *30*, 451–472. [CrossRef]
106. Razandi, Y.; Pourghasemi, H.R.; Neisani, N.S.; Rahmati, O. Application of Analytical Hierarchy Process, Frequency Ratio, and Certainty Factor Models for Groundwater Potential Mapping Using GIS. *Earth Sci. Inform.* **2015**, *8*, 867–883. [CrossRef]
107. Abo-Khomra, N.K.N.; Al-Tamimi, O.S.I.; Othman, A.A. DRASTIC for Groundwater Vulnerability Assessment Using GIS: A Case Study in Laylan Sub-Basin, Kirkuk, Iraq. *Iraqi Geol. J.* **2022**, 71–81. [CrossRef]